

---

# Ensembling Language Models with Sequential Monte Carlo

---

Robin S.M. Chan<sup>1</sup> Tianyu Liu<sup>1</sup> Samuel Kiegeland<sup>1,2</sup> Clemente Pasti<sup>1,2</sup> Jacob Hoover Vigly<sup>2</sup>  
 Timothy J. O’Donnell<sup>2,3,4,5</sup> Ryan Cotterell<sup>1</sup> Tim Vieira<sup>1</sup>

## Abstract

Practitioners have access to an abundance of language models and prompting strategies for solving many language modeling tasks; yet prior work shows that modeling performance is highly sensitive to both choices. Classical machine learning ensembling techniques offer a principled approach: aggregate predictions from multiple sources to achieve better performance than any single one. However, applying ensembling to language models during decoding is challenging: naively aggregating next-token probabilities yields samples from a locally normalized, biased approximation of the generally intractable ensemble distribution over strings. In this work, we introduce a unified framework for composing  $K$  language models into  $f$ -ensemble distributions for a wide range of functions  $f: \mathbb{R}_{\geq 0}^K \rightarrow \mathbb{R}_{\geq 0}$ . To sample from these distributions, we propose a byte-level sequential Monte Carlo (SMC) algorithm that operates in a shared character space, enabling ensembles of models with mismatching vocabularies and consistent sampling in the limit. We evaluate a family of  $f$ -ensembles across prompt and model combinations for various structured text generation tasks, highlighting the benefits of alternative aggregation strategies over traditional probability averaging, and showing that better posterior approximations can yield better ensemble performance.<sup>1</sup>

## 1. Introduction

Language models trained on different data, architectures, or objectives often exhibit complementary strengths. Even different prompts applied to the same model can surface distinct capabilities. The successes of ensemble methods

<sup>1</sup>ETH Zürich <sup>2</sup>CHI-FRO <sup>3</sup>McGill University <sup>4</sup>Mila <sup>5</sup>Canada CIFAR AI Chair. Correspondence to: Robin Chan <robin.chan@inf.ethz.ch>, Tim Vieira <tim.f.vieira@gmail.com>.

Preprint. March 6, 2026.

<sup>1</sup>Code: [https://github.com/chanr0/smc\\_ensembling](https://github.com/chanr0/smc_ensembling)

in classical machine learning motivate the application of various prediction aggregation strategies to combine the strengths of individual models into a single, better predictor. For instance, probability averaging in the traditional ensembling sense reduces variance (Jordan and Jacobs, 1994), the product of experts (Hinton, 1999) concentrates probability mass on regions of agreement, and other operations induce completely different behaviors (Kittler et al., 1998). Sampling from such ensemble distributions has practical applications in language modeling. For instance, *probability averaging* is most widely used to reduce variance and marginalize over individual model errors (see, *inter alia*, Liu et al., 2024; Yao et al., 2025); *contrastive* operators can be employed to “steer” generation, amplifying desirable traits while suppressing toxic or hallucinatory outputs (Liu et al., 2021; Li et al., 2023; Dekoninck et al., 2024); finally, the *product* between a language model and a constraint is often used for controlled generation, when the goal is to restrict output to the intersection of hard logical or syntactic constraints (Lipkin et al., 2025; Loula et al., 2025).

Applying these strategies to language models is not straightforward, as they define distributions over *sequences* of symbols, or *strings*, and generate these autoregressively. One commonly used strategy is to apply ensembling *during* decoding by aggregating next-token distributions at each generation step. Most prior work in this space has focused on the *vocabulary alignment problem*—combining models with mismatching tokenization—proposing various heuristics such as union vocabularies (Yu et al., 2024; Yao et al., 2025), or shared embedding spaces (Huang et al., 2024; Xu et al., 2024). Once token alignment is achieved, these methods predominantly default to (weighted) token probability averaging (cf. §A), sampling from locally normalized, biased approximations of the true global ensemble distribution over strings (Park et al., 2024). In this work, we sidestep the vocabulary alignment problem by mapping language models to the character level, which allows us to focus on different questions: beyond probability averaging, what ensembling strategies are effective, and what do we gain by consistently sampling from the *global* ensemble distribution over *strings* rather than local approximations?

We address these questions by introducing  $f$ -ensembles, a unified framework for composing  $K$  language models with

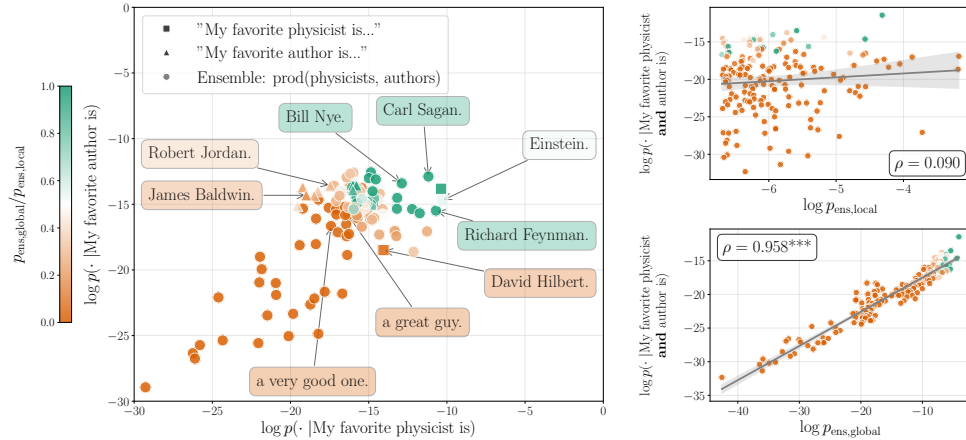


Figure 1. Prompt intersection on GPT-2. We generate 200 strings from the normalized token-level product of “My favorite physicist is” and “My favorite author is” prompts, then score each under the local ensemble  $p_{\text{ens,local}}$  (string probabilities emerging from locally normalized token-level product ensembling) and global ensemble  $p_{\text{ens,global}}$  (normalized product of string probabilities). Left: scatter plot of log probabilities with color indicating the generated strings’ global probability relative to their local ones. We also plot completions from the author prompt ( $\blacktriangle$ ) and the physicist prompt ( $\blacksquare$ ) that don’t overlap with the ensemble’s completions ( $\bullet$ ). Right: Correlation with the explicitly formulated intersection constraint probability  $p(\cdot \mid \text{“My favorite physicist and author is”})$ .

a wide range of ensembling functions  $f: \mathbb{R}_{\geq 0}^K \rightarrow \mathbb{R}_{\geq 0}$ . For inference, we propose a character-level sequential Monte Carlo algorithm, which enables the rigorous combination of models with mismatching tokenization and allows consistent sampling from the global  $f$ -ensemble distribution (i.e., in the limit). Our main empirical contribution is to evaluate and compare a diverse range of  $f$ -ensembles within the family of *generalized means* on a range of structured text generation tasks. We evaluate within-model prompt ensembling, as well as ensembles across model families. Our results demonstrate the efficacy of ensembles for improving base model performance and show a significant effect of the choice of ensembling function on task performance. Namely, we find that *consensus-seeking* strategies, such as the product, consistently outperform local probability averaging. Finally, we show the utility of our SMC ensembling algorithm by highlighting the performance improvements driven by better approximations of the global ensemble posterior.

## 2. Motivation: Global Prompt Intersection

We first motivate the utility of ensembling language models—and sampling from good ensemble posterior approximations—with a *prompt intersection* experiment adapted from Lew et al. (2023).

**Setup.** Consider a language model prompted with two prefixes with overlapping plausible completions. A practitioner may be interested in sampling strings that are probable under both prompts, i.e., sampling from their intersection. For illustrative purposes of this example, we prompt GPT-2 (Radford et al., 2019) with “My favorite physicist is” and

“My favorite author is” and aim to synthesize an ensemble that places high probability on physicists who are also authors. To that end, we generate 200 completions ending in a period using best-first beam search (beam width 20), scoring partial sequences by the cumulative, locally normalized product of next-token probabilities.

**String Scoring.** We compare two ways of scoring completions under the ensemble: (1)  $p_{\text{ens,local}}$ , which multiplies the token-level probabilities from each prompt at every generation step, then normalizes; and (2)  $p_{\text{ens,global}}$ , which first computes each prompt’s probability for the entire completed string, then multiplies these string-level probabilities. We normalize  $p_{\text{ens,global}}$  across the 200 generated completions.<sup>2</sup>

**Results.** In Figure 1, we plot the 200 ensemble completions ( $\bullet$ ) alongside completions generated from each prompt individually ( $\blacktriangle$  for authors,  $\blacksquare$  for physicists). We see that the completions generated from the locally normalized product ensemble tend to be ones that are assigned high probability under both prompts, rather than those probable under only one prompt (e.g., “James Baldwin”, a probable completion for the author prompt, is improbable under the physicist prompt, making it also low-probability under the ensemble). However, when comparing the probabilities assigned by the local ensemble with the global one, we observe a systematic mismatch: the local ensemble places relatively more probability mass on globally low-probability continuations, such as “a great guy.”, and relatively less probability on globally high-probability strings, such as “Carl Sagan.”.

<sup>2</sup>The true marginal likelihood is intractable, as it requires an infinite sum over all possible strings. However, these approximate probabilities only differ from the true ones by a constant.

This occurs because the local product rewards tokens that are individually probable under both prompts at each step—favoring generic continuations like “a” or “my” early on—rather than rewarding full completions that are probable for both prompts. A completion like “a great guy.” accumulates high local scores despite being improbable under the string-level global ensemble.

We validate this observation by scoring the generated completions under a prompt that explicitly encodes the intersection constraint: “My favorite physicist **and** author is”. The global ensemble probabilities strongly correlate with this explicit constraint ( $\rho = 0.958$ ,  $p < 0.001$ ), while the local ensemble does not ( $\rho = 0.090$ ,  $p = 0.24$ ).

**Insights.** This example illustrates two key points. First, global ensembling over strings can yield markedly different behavior than local token-level ensembling. In this example, the global product ensemble yields a significantly better approximation of the intended intersection constraint. Second, the product ensemble captures a meaningful property: concentrating probability on strings that are probable under both language models. However, it is only one aggregation strategy in the vast design space of aggregation functions that induce a variety of behaviors. In combination, these findings raise the question: Across the spectrum of behaviors induced by different ensembling functions  $f$ , how can we sample from their global distributions over strings?

### 3. Background: Language Models

An **alphabet**  $\Gamma$  is a finite, non-empty set of symbols. Let  $\Gamma^*$  denote the set of all strings  $\gamma$  formed from the symbols in  $\Gamma$ , including the empty string  $\varepsilon$ . We write  $|\gamma|$  to denote the length of  $\gamma$ . A **language model**  $p$  is a probability distribution over  $\Gamma^*$ . We write  $\Delta^{\Gamma^*}$  to denote the set of valid probability distributions (language models) over  $\Gamma^*$ .

Let  $\gamma' \succeq \gamma$  denote that  $\gamma$  is a prefix of  $\gamma'$ . The **prefix probability**  $\bar{p}(\gamma)$  is the probability that a string drawn from  $p$  begins with  $\gamma \in \Gamma^*$ :

$$\bar{p}(\gamma) \stackrel{\text{def}}{=} \sum_{\gamma' \in \Gamma^*} p(\gamma \gamma') \quad (1)$$

For every  $\gamma, \gamma' \in \Gamma^*$  where  $\bar{p}(\gamma) > 0$ , we define the **conditional prefix probability**

$$\bar{p}(\gamma' | \gamma) \stackrel{\text{def}}{=} \begin{cases} \frac{p(\gamma')}{\bar{p}(\gamma)} & \text{if } \gamma' = \gamma \square \\ \frac{\bar{p}(\gamma \gamma')}{\bar{p}(\gamma)} & \text{otherwise} \end{cases} \quad (2)$$

where  $\square$  denotes a distinguished **end-of-string** delimiter.<sup>3</sup> Note that  $\bar{p}(\cdot | \gamma)$  describes a probability distribution over

<sup>3</sup>Note that  $\square \notin \Gamma$ , and it is an error to append  $\square$  to any string.

$\Gamma \cup \{\square\}$ . Then, the probability of  $\gamma$  under language model  $p$  may be factorized as

$$p(\gamma) = \bar{p}(\square | \gamma) \underbrace{\prod_{t=1}^{|\gamma|} \bar{p}(\gamma_t | \gamma_{<t})}_{=\bar{p}(\gamma)} \quad (3)$$

This factorization corresponds to the generative process used by autoregressive language models, generating a string by iteratively appending samples from next-token distributions and stopping when  $\square$  is reached.

## 4. Language Model $f$ -Ensembles

Ensembling is a technique for combining *potential functions* (which may or may not be probability distributions) into a probability distribution that reflects some aspect of each. In particular, given a set of potentials  $p_1, \dots, p_K : \Sigma^* \rightarrow \mathbb{R}_{\geq 0}$ , defined over the character alphabet  $\Sigma$ ,<sup>4</sup> and the *ensemble function*  $f : \mathbb{R}_{\geq 0}^K \rightarrow \mathbb{R}$ , we define the  $f$ -ensemble as follows

**Definition 4.1.** The  $f$ -ensemble of potentials  $p_1, \dots, p_K \in \mathbb{R}_{\geq 0}^{\Sigma^*}$  is a distribution  $\Phi \in \Delta^{\Sigma^*}$  defined as

$$\Phi(\mathbf{x}) \stackrel{\text{def}}{=} \frac{f(p_1(\mathbf{x}), \dots, p_K(\mathbf{x}))}{Z} \\ Z \stackrel{\text{def}}{=} \sum_{\mathbf{x}' \in \Sigma^*} f(p_1(\mathbf{x}'), \dots, p_K(\mathbf{x}'))$$

for every  $f : \mathbb{R}_{\geq 0}^K \rightarrow \mathbb{R}$ , such that  $0 < Z < \infty$ . We further define  $\varphi(\mathbf{x}) \stackrel{\text{def}}{=} f(p_1(\mathbf{x}), \dots, p_K(\mathbf{x}))$  as the **unnormalized ensemble distribution**.

Since  $\Phi$  is a probability distribution, the prefix probability  $\vec{\Phi}$  and the conditional prefix probability  $\vec{\Phi}(\mathbf{x}' | \mathbf{x})$  follow directly from Eq. (1). Ideally, to sample from  $\Phi$  we would iteratively sample from the conditional next-symbol probability  $\vec{\Phi}(x_t | \mathbf{x}_{<t})$ , with  $x_t \in (\Sigma \cup \square)$ , until the end of sequence delimiter  $\square$  is hit. However, sampling directly from  $\vec{\Phi}(x_t | \mathbf{x}_{<t})$  is often unfeasible as computing  $Z$  is intractable. Therefore, in §5 we explore various strategies to approximately sample from  $\vec{\Phi}(x_t | \mathbf{x}_{<t})$ .

### 4.1. A Family of $f$ -Ensembles

Definition 4.1 admits a wide range of aggregation functions  $f$ —but which should we choose? We show that the *family*

<sup>4</sup>Note that, when  $\{p_k\}_{k=1}^K$  are defined over different token alphabets, a common issue is *tokenization mismatch*, i.e., when two potentials do not share the same alphabet, token level probabilities cannot be aggregated directly. We address this by mapping each model to a shared probability space, defined on the common character alphabet  $\Sigma$ . This problem was discussed in detail by Vieira et al. (2025a), for further details regarding the specific setting of this paper, see §C.

Table 1. The generalized means family of  $f$ -ensembles. The ensemble  $\Phi$  minimizes  $\sum_{k=1}^K w_k D_\alpha(\Phi \parallel p_k)$ . The divergences are defined as: Pearson  $\chi^2$ :  $D_{\chi^2}(p \parallel q) \stackrel{\text{def}}{=} \sum_{\mathbf{x} \in \Sigma^*} \frac{(p(\mathbf{x}) - q(\mathbf{x}))^2}{q(\mathbf{x})}$ ; KL:  $D_{\text{KL}}(p \parallel q) \stackrel{\text{def}}{=} \sum_{\mathbf{x} \in \Sigma^*} p(\mathbf{x}) \log \frac{p(\mathbf{x})}{q(\mathbf{x})}$ ; and Rényi- $\infty$ :  $D_\infty(p \parallel q) \stackrel{\text{def}}{=} \log \max_{\mathbf{x} \in \Sigma^*} \frac{p(\mathbf{x})}{q(\mathbf{x})}$ .

	$\tau$	Name	$f$ -Ensemble	Minimized $D_\alpha$
consensus	$-\infty$	Minimum	$\frac{1}{Z} \min_{k=1}^K p_k(\mathbf{x})$	$D_\infty(\Phi \parallel p_k)$
	$-1$	Harmonic	$\frac{1}{Z} \left( \sum_{k=1}^K \frac{w_k}{p_k(\mathbf{x})} \right)^{-1}$	$D_{\chi^2}(\Phi \parallel p_k)$
	$0$	Product	$\frac{1}{Z} \prod_{k=1}^K p_k(\mathbf{x})^{w_k}$	$D_{\text{KL}}(\Phi \parallel p_k)$
coverage	$1$	Sum	$\frac{1}{Z} \sum_{k=1}^K w_k p_k(\mathbf{x})$	$D_{\text{KL}}(p_k \parallel \Phi)$
	$2$	Quadratic	$\frac{1}{Z} \sqrt{\sum_{k=1}^K w_k p_k(\mathbf{x})^2}$	$D_{\chi^2}(p_k \parallel \Phi)$
	$+\infty$	Maximum	$\frac{1}{Z} \max_{k=1}^K p_k(\mathbf{x})$	$D_\infty(p_k \parallel \Phi)$

of *generalized means* arises naturally from a variational principle: they are the unique minimizers of weighted sums of  $\alpha$ -divergences to the base potentials.

Specifically, consider  $K$  expert potentials  $\{p_k\}_{k=1}^K$ , where  $p_k : \Sigma^* \rightarrow \mathbb{R}_{\geq 0}$ . Our goal is to construct a single ensemble distribution  $\Phi$  that synthesizes the information provided by the  $K$  experts, given prior expert weights  $\mathbf{w} \in \Delta^K$ . Following prior work by Dekoninck et al. (2024), we define the *optimal* consensus distribution  $\Phi^*(\mathbf{x})$  minimizing a weighted sum of divergences  $D$ , i.e.,

$$\Phi^* \stackrel{\text{def}}{=} \underset{\Phi \in \Delta^{\Sigma^*}}{\text{argmin}} \sum_{k=1}^K w_k D(\Phi \parallel p_k) \quad (4)$$

The choice of  $D$  determines how similarity between distributions is assessed and, therefore, influences which ensemble distribution is considered optimal. In this work, we discuss  $D$  within the family of  $\alpha$ -divergences (Amari, 1985):

$$D_\alpha(q \parallel p) = \frac{1}{\alpha(1-\alpha)} \left( 1 - \sum_{\mathbf{x} \in \Sigma^*} q(\mathbf{x})^\alpha p(\mathbf{x})^{1-\alpha} \right) \quad (5)$$

**Theorem 4.1** ( $\alpha$ -Divergence Ensembles). *Let  $D_\alpha$  be the  $\alpha$ -divergence with parameter  $\alpha \in \mathbb{R} \setminus \{0, 1\}$ . The unique consensus distribution  $\Phi^*$  that minimizes the expert-weighted loss in Eq. (4) is the **generalized mean** of the experts, with power parameter  $\tau \stackrel{\text{def}}{=} 1 - \alpha$ :*

$$\Phi^*(\mathbf{x}) = \frac{1}{Z} \left( \sum_{k=1}^K w_k p_k(\mathbf{x})^\tau \right)^{\frac{1}{\tau}} \quad (6)$$

where  $Z$  is the normalizer ensuring  $\sum_{\mathbf{x} \in \Sigma^*} \Phi^*(\mathbf{x}) = 1$ .

*Proof.* In Appendix D. ■

## Qualitative analysis of generalized mean ensembles.

Generalized means unify many practically used model aggregation strategies under a single framework, recovering product of experts (Hinton, 1999; 2002) as  $\tau \rightarrow 0$ , mixture of experts (Jordan and Jacobs, 1994) as  $\tau \rightarrow 1$ , and min and max aggregations (Kittler et al., 1998) as  $\tau \rightarrow \pm\infty$ . Deriving them as minimizers of weighted sums of  $\alpha$ -divergences further explains how these methods mediate disagreements between experts, and provides a qualitative guide for choosing  $f$  (cf. Tab. 1). The regime where  $\tau \leq 0$  exhibits *consensus-seeking* behavior (where  $p_k(\mathbf{x}) = 0 \rightarrow \Phi(\mathbf{x}) = 0$ ), which forces the ensemble to concentrate probability mass on the intersection of the expert supports. In contrast, the regime where  $\tau \geq 1$  exhibits *coverage-seeking* behavior (where  $p_k(\mathbf{x}) > 0 \rightarrow \Phi(\mathbf{x}) > 0$ ), forcing the ensemble to distribute mass over the union of the expert supports. In both regimes,  $|\tau|$  modulates the effect’s strength.

## 5. Approximate Inference

We now describe how to (approximately) sample from any  $f$ -ensemble distribution  $\Phi$ . The strategies we present are different instantiations of *importance sampling* (Robert and Casella, 2005). In general, we will approximately sample from  $\Phi$ —which is generally intractable—by sampling from a tractable *proposal* distribution and appropriately correcting the resulting distortion with an *importance weight*. Adopting the importance sampling terminology, we will refer to  $\Phi$  as the *target distribution*, and to  $\varphi$  as the *unnormalized target*.

### 5.1. Importance Sampling

Importance sampling is a general-purpose technique for approximating intractable distributions. We now present a version adapted to the special case of estimating  $f$ -ensembles:

**Definition 5.1.** *Importance sampling works as follows: Given a sample budget  $M > 0$ ,<sup>5</sup> we sample  $\mathbf{x}^{(1)}, \dots, \mathbf{x}^{(M)} \stackrel{\text{i.i.d.}}{\sim} r$  from a **proposal distribution**  $r \in \Delta^{\Sigma^*}$ .<sup>6</sup> We associate an **importance weight** with each  $\mathbf{x}^{(m)}$ , i.e.,  $w^{(m)} \stackrel{\text{def}}{=} \varphi(\mathbf{x}^{(m)})/r(\mathbf{x}^{(m)})$ . We then define the **estimated unnormalized target**:*

$$\widehat{\varphi}(\mathbf{x}) \stackrel{\text{def}}{=} \frac{1}{M} \sum_{m=1}^M w^{(m)} \mathbb{1}\{\mathbf{x} = \mathbf{x}^{(m)}\} \quad (7)$$

*The estimated target distribution alongside the estimated*

<sup>5</sup>Chatterjee and Diaconis (2018) show that the number of samples required for importance sampling with proposal distribution  $r$  to obtain a *good* approximation of the target distribution  $\Phi$  is exponential in the KL divergence  $\text{KL}(\Phi \parallel r)$ .

<sup>6</sup>For technical reasons, we require  $r$  to satisfy  $\varphi(\mathbf{x}) > 0 \implies \Phi(\mathbf{x}) > 0$  for all  $\mathbf{x} \in \Sigma^*$ , or equivalently (by contrapositive)  $\Phi(\mathbf{x}) = 0 \implies \varphi(\mathbf{x}) = 0$  for all  $\mathbf{x} \in \Sigma^*$ . We provide a discussion about the implications in §D.2.

normalization constant are given as:

$$\widehat{\Phi}(\mathbf{x}) \stackrel{\text{def}}{=} \frac{\widehat{\varphi}(\mathbf{x})}{\widehat{Z}}, \quad \widehat{Z} \stackrel{\text{def}}{=} \frac{1}{M} \sum_{m=1}^M w^{(m)} \quad (8)$$

Crucially, importance sampling provides an *unbiased* estimate  $\widehat{Z}$  of the normalizing constant  $Z$ , and an estimate  $\widehat{\Phi}$  of the ensemble distribution  $\Phi$  that is *consistent* (but biased for finite  $M$ ). See §D.1 for more details and proofs of correctness. Importance sampling of complete strings is not well-suited to an autoregressive language model, which is inherently a sequential model. For this reason, we introduce sequential importance sampling.

## 5.2. Sequential Importance Sampling

Sequential importance sampling (SIS; Del Moral et al., 2006) is a variant of importance sampling designed for distributions over sequences, where samples are built incrementally by extending partial sequences according to a proposal kernel. In language modeling, this kernel is typically the next-token distribution (cf. Eq. (3)), which extends a partial string by one symbol at each step. At each time step, the importance weights are updated, yielding in the end an importance weight for each *particle* as in Def. 5.1.<sup>7</sup> In order to compute the weight update, we need to have access to the *next token prefix target*:

$$\vec{\varphi}(x' | \mathbf{x}) \stackrel{\text{def}}{=} \begin{cases} \frac{\varphi(\mathbf{x})}{\vec{\varphi}(\mathbf{x})} & \text{if } x' = \square \\ \frac{\vec{\varphi}(\mathbf{x}x')}{\vec{\varphi}(\mathbf{x})} & x' \in \Sigma \end{cases} \quad (9)$$

where  $\vec{\varphi}(\mathbf{x}) \stackrel{\text{def}}{=} \Phi(\mathbf{x}) \cdot Z$ . Unfortunately,  $\vec{\varphi}$  is itself intractable.<sup>8</sup> Therefore, we introduce a **shaping function**  $\vec{\psi}: \Sigma^* \rightarrow \mathbb{R}_{\geq 0}$  as an *intermediate target* to compute the importance weights. A common choice for  $\vec{\psi}(\mathbf{x})$  is  $f(\vec{p}_1(\mathbf{x}), \dots, \vec{p}_K(\mathbf{x}))$ , which, notably, is not the same as  $\vec{\varphi}(\mathbf{x})$ . Intuitively, the shaping function serves as a tractable surrogate for the intractable prefix target, guiding the sampler towards promising regions of  $\Sigma^*$ .

To compute the importance weight update for SIS, we need to define a next-token version of the shaping function:<sup>9</sup>

$$\vec{\psi}(x' | \mathbf{x}) \stackrel{\text{def}}{=} \begin{cases} \frac{\varphi(\mathbf{x})}{\vec{\psi}(\mathbf{x})} & \text{if } x' = \square \\ \frac{\vec{\psi}(\mathbf{x}x')}{\vec{\psi}(\mathbf{x})} & \text{otherwise} \end{cases} \quad (10)$$

Importantly, this definition gives the following factorization of  $\varphi$ ,  $\forall \mathbf{x} \in \Sigma^*$  (which preserves the importance weights);

$$\varphi(\mathbf{x}) = \vec{\psi}(\varepsilon) \vec{\psi}(\square | \mathbf{x}) \prod_{t=1}^{|\mathbf{x}|} \vec{\psi}(x_t | \mathbf{x}_{<t}) \quad (11)$$

<sup>7</sup>Samples are often called *particles* in SIS.

<sup>8</sup>It would require computing an infinite sum  $\sum_{\mathbf{x}' \in \Sigma^*} f(p_1(\mathbf{x} \mathbf{x}'), \dots, p_K(\mathbf{x} \mathbf{x}'))$ .

<sup>9</sup>Note that  $\vec{\psi}(\cdot | \mathbf{x})$  is not necessarily a probability distribution.

**Proposition 5.1.** *The shaping weights are equivalent to those used in importance sampling:*

$$\frac{\varphi(\mathbf{x})}{r(\mathbf{x})} = \vec{\psi}(\varepsilon) \frac{\vec{\psi}(\square | \mathbf{x})}{\vec{r}(\square | \mathbf{x})} \prod_{t=1}^{|\mathbf{x}|} \frac{\vec{\psi}(x_t | \mathbf{x}_{<t})}{\vec{r}(x_t | \mathbf{x}_{<t})} \quad (12)$$

*Proof.* Prop. 5.1 follows directly from Eq. (11) and Eq. (3) applied to  $r(\mathbf{x})$ , followed by algebra. ■

Interestingly, it turns out that the optimal choice for the proposal distribution is proportional to the shaping itself:

**Proposition 5.2.** *The locally optimal proposal distribution i.e., the one that minimizes the variance of the importance weight update at each step, is  $\vec{r}^*(x' | \mathbf{x}) \propto \vec{\psi}(x' | \mathbf{x})$ .*

See §D.1 for proof. Note that, even when the proposal is proportional to the next-token shaping function, the two may still differ when the shaping function is not normalized.

---

### Algorithm 1 Sequential Monte Carlo<sup>10</sup>

---

1. **procedure** SMC( $r, \vec{\psi}, M, \tau$ )
  2.   **for**  $m = 1 \dots M$  : ▷  $M$  number of samples
  3.      $(\mathbf{x}^{(m)}, w^{(m)}, \alpha^{(m)}) \leftarrow (\varepsilon, \vec{\psi}(\varepsilon), \text{true})$
  4.   **while**  $\exists m \in 1 \dots M$  :  $\alpha^{(m)}$  :
  5.     **for**  $m = 1 \dots M$  such that  $\alpha^{(m)}$  : ▷ Active particles
  6.        $y' \sim r(\cdot | \mathbf{x}^{(m)})$
  7.       **if**  $y' = \square$  : ▷ Complete the particle
  8.          $\alpha^{(m)} \leftarrow \text{false}$
  9.       **else**
  10.          $\mathbf{x}^{(m)} \leftarrow \mathbf{x}^{(m)} \circ y'$
  11.          $w^{(m)} \leftarrow w^{(m)} \frac{\vec{\psi}(y' | \mathbf{x}^{(m)})}{r(y' | \mathbf{x}^{(m)})}$
  12.          $(\mathbf{x}^{(\cdot)}, w^{(\cdot)}, \alpha^{(\cdot)}) \leftarrow \text{RESAMPLE}(\mathbf{x}^{(\cdot)}, w^{(\cdot)}, \alpha^{(\cdot)}, \tau)$
  13.          $\widehat{Z} \leftarrow \frac{1}{M} \sum_{m=1}^M w^{(m)}$
  14.          $\widehat{\varphi}(\mathbf{x}) \leftarrow \frac{1}{M} \sum_{m=1}^M w^{(m)} \mathbb{1}\{\mathbf{x} = \mathbf{x}^{(m)}\}$
  15.          $\widehat{\Phi}(\mathbf{x}) \leftarrow \frac{\widehat{\varphi}(\mathbf{x})}{\widehat{Z}}$
  16.       **return**  $(\widehat{Z}, \widehat{\varphi}, \widehat{\Phi})$
  17. **procedure** RESAMPLE( $\mathbf{x}^{(\cdot)}, w^{(\cdot)}, \alpha^{(\cdot)}, \tau$ )
  18.    $W \leftarrow \sum_{m=1}^M w^{(m)}$
  19.    $\widehat{M} \leftarrow W^2 / \left( \sum_{m=1}^M (w^{(m)})^2 \right)$
  20.   **if**  $\widehat{M} < \tau \cdot M$  : ▷ Resample
  21.      $\bar{\mathbf{x}}^{(\cdot)} \leftarrow \mathbf{x}^{(\cdot)}; \bar{w}^{(\cdot)} \leftarrow w^{(\cdot)}$  ▷ Temporary copy
  22.     **for**  $m = 1 \dots M$  :
  23.        $R \sim \text{Categorical}(W^{-1} \langle \bar{w}^{(1)}, \dots, \bar{w}^{(M)} \rangle)$
  24.        $(\mathbf{x}^{(m)}, w^{(m)}, \alpha^{(m)}) \leftarrow (\bar{\mathbf{x}}^{(R)}, W/M, \alpha^{(R)})$
  25.     **return**  $(\mathbf{x}^{(\cdot)}, w^{(\cdot)}, \alpha^{(\cdot)})$
- 

<sup>10</sup>Note that the final weight step is more detailed than the pseudocode suggests, as  $\square$  is handled as in Eq. (10).

### 5.3. Sequential Monte Carlo

Sequential Monte Carlo (SMC) is a generalization of SIS that incorporates a resampling step that reallocates computation from less to more promising partial sequences while sampling particles. More concretely, using a multinomial resampling strategy, at each step,<sup>11</sup> SMC samples indices  $a^{(1)}, \dots, a^{(M)} \stackrel{\text{i.i.d.}}{\sim} \text{Categorical}(W^{-1}\langle w^{(1)}, \dots, w^{(M)} \rangle)$ , where  $W \stackrel{\text{def}}{=} \sum_{m=1}^M w^{(m)}$ . All particles are then reassigned as  $(\mathbf{x}^{(i)}, w^{(i)}) = (\mathbf{x}^{(a^{(i)})}, W/M)$ . The full procedure is shown in Alg. 1.

## 6. Experiments

Different LMs and prompts often exhibit complementary strengths on the same task (Polo et al., 2024). As discussed in our related work section (cf. §A), prior work on LM ensembling during inference has largely focused on local probability averaging (i.e., sum ensembles) (Yao et al., 2025), whereas our  $f$ -ensemble framework spans a broader family of aggregation strategies. We evaluate whether these alternative  $f$ -ensembles can exploit this to improve upon individual models across tasks. More specifically, our experiments aim to answer the following questions:

- RQ1. To what extent can language models be *synergistic*, i.e., work better jointly, rather than on their own?
- RQ2. In what ways does the mediation strategy between models, encoded by  $f$ , affect performance under the resulting ensemble?
- RQ3. How does the quality of approximation of  $\Phi$  affect the performance of the  $f$ -ensemble?

### 6.1. Setup

**Models and Prompts.** We evaluate ensembles using instruction-tuned LMs from three model families: Llama (Llama3.1-8B-Instruct; Llama Team, 2024), Qwen (Qwen2.5-7B-Instruct; Yang et al., 2025), and Phi (phi-4 (14B); Abdin et al., 2024). This yields two experimental settings: *within-model* ensembles that combine the same model under different prompts and *cross-model* ensembles that combine two models under the same prompt.

**Datasets.** We study the effectiveness of ensembling language models on three exact-match structured text generation tasks in different domains, where the number of generation steps allows differences between local and global sampling to manifest. For each dataset, we evaluate 100 randomly sampled instances.

<sup>11</sup>In practice, resampling is only done based on the **effective sample size**  $\hat{N} \stackrel{\text{def}}{=} \frac{(\sum_{m=1}^M w^{(m)})^2}{\sum_{m=1}^M (w^{(m)})^2}$  which measures the variance among importance weights. We resample when  $\hat{N}$  falls below a threshold  $\tau \cdot M$  for  $\tau \in (0, 1)$ .

- **JSON.** *Task:* Generate documents that conform to a specific JSON schema using the GlaiVeAI function-calling dataset (GlaiveAI, 2024) from JSONSchemaBench (Geng et al., 2025). *Metric:* Binary correctness, whether the generated string conforms to a specific JSON schema.
- **Big-Bench Hard.** *Task:* Diverse reasoning tasks (Suzgun et al., 2023). We focus on the word sorting subtask: given a list of words, sort them in alphabetical order. *Metric:* binary correctness of the generated sorted list.
- **Text-to-SQL.** *Task:* Generate SQL queries from a natural language question and relevant database schema (Yu et al., 2018). *Metric:* Execution accuracy, i.e., checking whether the generated query produces the same output when executed against the provided test database.

**Baselines.** In this work, we study which aggregation functions effectively combine models and how approximation quality affects performance. Notably, as discussed in §A, these questions are largely orthogonal to improving model routing, enhancing post-hoc selection (e.g., best-of- $N$ ), or comparing vocabulary alignment heuristics. Thus, to evaluate RQ1-RQ3, we compare our SMC  $f$ -ensembles against: (1) the best-performing base model, (2) locally normalized probability averaging (the predominant aggregation strategy for ensembling during inference; Chen et al., 2025), (3)  $f$ -ensembles at different approximation qualities, notably, locally normalized  $f$ -ensembles.

**Evaluation Metric.** Because a  $f$ -ensemble defines a distribution over outputs, we evaluate its performance in terms of the probability mass it assigns to correct answers, i.e., accuracy in expectation under  $\Phi$ , rather than the accuracy of a single decoded output. We approximate it using the weighted particles from SMC:

$$\mathbb{E}_{\mathbf{x} \sim \Phi} [\mathbb{1}\{\mathbf{x} \in \mathcal{Y}\}] \approx \sum_{m=1}^M \bar{w}^{(m)} \cdot \mathbb{1}\{\mathbf{x}^{(m)} \in \mathcal{Y}\} \quad (13)$$

where  $\bar{w}^{(m)} = w^{(m)} / \sum_{m'=1}^M w^{(m')}$  are the normalized importance weights and  $\mathcal{Y} \subseteq \Sigma^*$  is the set of correct outputs.

**$f$ -Ensembles.** We evaluate four generalized means spanning the consensus-coverage spectrum: min of experts ( $\tau \rightarrow -\infty$ ), product of experts ( $\tau = 0$ ), mixture of experts ( $\tau = 1$ ), and max of experts ( $\tau \rightarrow \infty$ ). These represent commonly used aggregation strategies (Khalifa et al., 2023) and the meaningful limits of the generalized mean family (see Tab. 1), enabling systematic analysis of how the choice of aggregation affects performance. The used functions are *annihilative*<sup>12</sup>, ensuring the used shaping function (cf. §5.2) satisfies absolute continuity when used as the proposal.

Across experiments, we report means and 95% CIs across 5 different seeds with  $M = 10$  particles (we provide particle ablations in §G.3), a resampling threshold of 0.9, and equal

<sup>12</sup>In fact, all generalized means are, as derived in Prop. D.2.

Table 2. Summary of model ensembling results. **Bold**: non-overlapping 95% CIs with best baseline. †: highest average expected accuracy by column (within-model), or overall (cross-model). Shaded: strongest single-prompt baseline.

Method	JSON Schema			BBH (Word Sorting)			SPIDER (Text-to-SQL)		
	Qwen	Phi	Llama	Qwen	Phi	Llama	Qwen	Phi	Llama
Prompt 1	95.6±0.8	83.5±1.9	86.3±1.6	13.9±1.0	27.7±1.2	38.6±1.5	40.0±1.5	24.2±1.5	38.4±1.8
Prompt 2	93.8±0.9	79.5±5.6	84.3±2.5	5.8±0.9	24.3±1.5	36.5±1.9	53.6±1.0†	34.5±1.7	36.3±1.7
Local Prob. Avg.	95.2±3.2	82.0±4.7	83.4±3.5	9.6±3.0	25.8±5.8	41.2±6.5	45.6±3.7	28.4±4.8	39.4±6.3
Best Local $f$ -Ens.	96.4±0.7†	87.2±4.4	88.6±4.4	15.0±2.3	27.2±5.1	<b>45.0±2.9†</b>	52.6±1.4	36.0±3.4†	<b>43.6±3.4†</b>
Best Global $f$ -Ens. (Token SMC, $M = 10$ )	96.0±0.2	<b>87.4±0.3</b>	88.9±1.1	<b>15.3±2.0</b>	28.2±1.1	<b>42.3±0.9</b>	51.2±1.8	34.2±0.7	<b>41.9±1.4</b>
Best Global $f$ -Ens. (Token SMC, $M = 25$ )	95.8±0.3	<b>87.8±0.8†</b>	<b>89.1±0.4†</b>	<b>14.9±1.3</b>	28.6±1.0†	<b>42.7±0.6</b>	51.2±0.9	34.5±0.7	<b>42.0±0.5</b>
Best Global $f$ -Ens. (Byte SMC, $M = 10$ )	92.8±1.0	<b>87.5±0.7</b>	88.9±1.4	<b>15.5±0.1†</b>	23.8±1.5	34.0±1.4	48.3±2.1	34.5±0.9	<b>42.4±0.9</b>
Best Cross-Model $f$ -Ens. (Byte SMC, $M = 10$ )	92.6±0.9(Q+P, Prompt 1)			41.1±1.0(P+L, Prompt 1)			55.5±1.1†(Q+L, Prompt 2)		

expert weight, unless specified otherwise. To understand the interactions between base models and the resulting ensemble distribution, we run our experiments for  $K = 2$  experts. We report more details in §E.

## 6.2. Results

### [RQ1] Models can act synergistically with themselves and each other.

The effectiveness of ensembling depends on how the experts differ: we empirically find that ensembles improve upon base models primarily when both prompts perform moderately on the same examples. When one prompt already succeeds, the other has little to contribute; when both fail, combining them does not help.<sup>13</sup> Accordingly, we introduce variation by selecting prompt pairs that provide complementary instructions (see §F for details). As shown in Table 5, this can already yield significant performance improvements over the better base model for at least one ensemble for each task.

Cross-model ensembles show similar increases in expected accuracy without requiring complementary prompt construction. For BBH and SPIDER, ensembling the two better-performing models with the same prompt yields significant improvements over base model performance—showing the ability to even outperform the best prompt ensembles. This suggests that architectural and data diversity across model families provides value beyond prompt variation alone.

### [RQ2] Consensus-seeking ensembles improve expected accuracy over probability averaging.

From Figure 2 (and more detailed results in Table 5), we also observe significant differences between ensemble methods across tasks and models. Although some significant variation is visible among operators (with min ensembles coming out on top most of the time), the primary distinction is between

<sup>13</sup>We provide empirical support in §G.2.

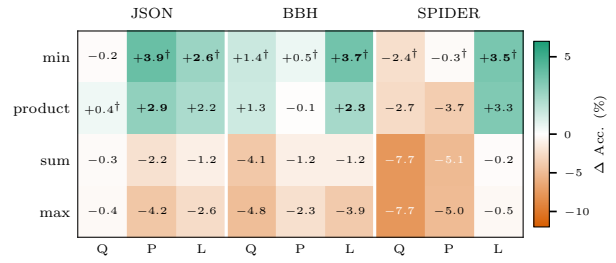


Figure 2.  $f$ -ensembles for token-level SMC. Values show change in accuracy (%) relative to the best single-prompt baseline. †: best in column. **Bold**: significant improvement over the best base prompt (non-overlapping 95% CIs). Q=Qwen, P=Phi, L=Llama.

consensus-seeking and coverage-seeking operators. In the setting of combining two complementary language models, consensus-seeking operators consistently outperform coverage-seeking ones. Additionally, in terms of expected accuracy, token-wise SMC ensembling with consensus-seeking operators yields significantly increased expected accuracies over the base model performances for at least one model per dataset. To better understand these results, we note that for any weighted mixture  $\Phi(\mathbf{x}) = \sum_{k=1}^K w_k p_k(\mathbf{x})$  with  $w \in \Delta^K$ , the ensemble’s expected accuracy is bounded by the better-performing base model:

$$\mathbb{E}_{\mathbf{x} \sim \Phi} [\mathbb{1}\{\mathbf{x} \in \mathcal{Y}\}] = \sum_{\mathbf{x} \in \Sigma^*} \Phi(\mathbf{x}) \cdot \mathbb{1}\{\mathbf{x} \in \mathcal{Y}\} \quad (14a)$$

$$= \sum_{k=1}^K w_k \mathbb{E}_{\mathbf{x} \sim p_k} [\mathbb{1}\{\mathbf{x} \in \mathcal{Y}\}] \quad (14b)$$

$$\leq \max_{k=1, \dots, K} \left( w_k \mathbb{E}_{\mathbf{x} \sim p_k} [\mathbb{1}\{\mathbf{x} \in \mathcal{Y}\}] \right) \quad (14c)$$

For an equal weighting (i.e., probability averaging),  $\mathbb{E}_{\mathbf{x} \sim \Phi} [\mathbb{1}\{\mathbf{x} \in \mathcal{Y}\}]$  equals the arithmetic mean of the base model accuracies.

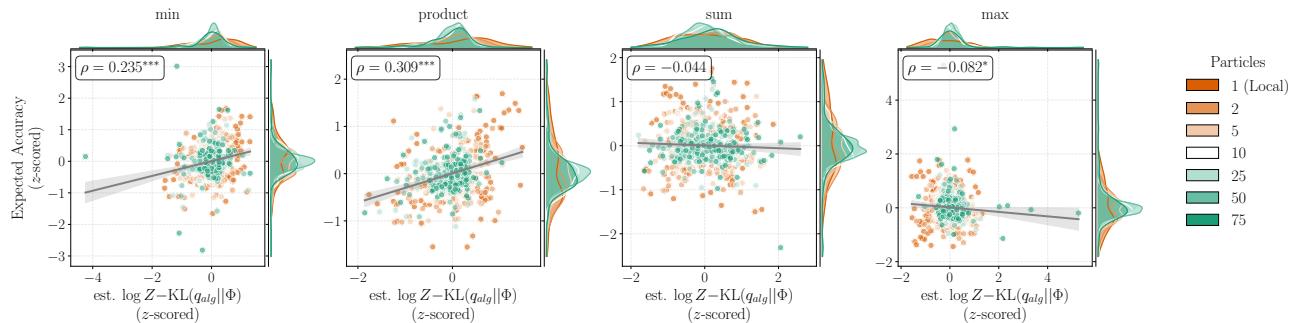


Figure 3. Representative relationship between expected accuracy and the estimated log marginal likelihood,  $\log \hat{Z}$ , on BBH for Llama. Each datapoint represents (sample, particle) configurations aggregated across seeds. Both metrics are  $z$ -scored per example to normalize for variations in problem difficulty and scale. Points are colored by the number of particles used for estimation. Marginal plots display the kernel density estimates for the respective axes. The grey line and shaded band indicate a linear regression fit with a 95% confidence interval. Pearson correlation coefficients  $\rho$  are annotated in the top-left (\*\*\* $p < 0.001$ , \* $p < 0.05$ ).

First, this provides a sanity check of our implementation: using our SMC algorithm, we observe that the expected accuracy of the equally-weighted mixture converges to the average accuracy of the base models as we increase the number of particles (cf. Table 5). Second, this observation yields a theoretical explanation for prior empirical work by Yao et al. (2025), which shows that if base LMs exhibit a large performance gap, a variety of LM ensembling methods that rely on local probability averaging drop below the accuracy of the better-performing model. We reproduce similar behavior in the local probability averaging baseline in Table 2. Although the locally normalized sampling distribution can differ from the global one used in our derivation, we see that probability averaging remains fundamentally constrained by this property, regardless of the performance gap. By contrast, consensus-seeking operators show more robust results.

**[RQ3] Approximation quality affects  $f$ -ensemble performance differently.** Table 2 shows some promising aggregated results regarding the usefulness of SMC for attaining better ensembles over baseline approaches. However, it remains unclear in what scenarios improved *approximation quality*, i.e., the closeness of our sampling distribution to the target distribution  $\Phi$ , correlates with expected accuracy in the evaluated tasks.

To this end, we follow prior work (Andrieu and Roberts, 2009; Lew et al., 2023; Zhao et al., 2024), which shows that  $\mathbb{E}[\log \hat{Z}]$  provides a lower bound on  $\log Z - \text{KL}(q_{\text{alg}} \parallel \Phi)$ , where  $q_{\text{alg}}$  denotes the marginal distribution induced by the SMC sampling algorithm. Intuitively, higher values of  $\mathbb{E}[\log \hat{Z}]$  mean that the algorithm’s samples are “better”, i.e., closer to being sampled from the global ensemble  $\Phi$ .

Both the approximation quality metric and expected accuracy are defined at the instance level, as  $\log Z$  varies across samples. To enable comparison, we compute per-instance Spearman correlations and report their mean in Table 6. For

visualization, we  $z$ -score both metrics per instance to normalize for problem difficulty, allowing us to plot aggregated trends. We visualize a representative subset in Figure 3, where we plot  $z$ -scored approximation quality against  $z$ -scored expected accuracy for each unique (sample, particle count) configuration aggregated across seeds, and refer to §G for additional results.

We observe rather consistent, medium-sized, significant positive Spearman correlations for consensus-seeking operators (min and product), which can also be seen in other datasets. This may suggest that for these  $f$ -ensembles, improving the posterior approximation, whether through additional particles or better proposals, translates to measurably higher task performance. In contrast, coverage-seeking operators (sum and max) tend to even show weak negative correlations between the approximation quality and expected accuracy. For sum ensembles, this aligns with our theoretical expectations, as, although local probability averaging can help, the global ensemble’s expected accuracy will always converge to the average of the base models’.

## 7. Conclusion

We develop  $f$ -ensembling; a unified framework for composing language models into ensemble distributions over strings. Motivated by significant differences in locally and globally normalized string scoring in prompt intersection, we further propose a flexible byte-level SMC ensembling algorithm that prioritizes globally promising samples during inference. In a series of experiments, we show that language models can act synergistically with one another. Unlike probability averaging, which is bounded by its base model performances, consensus-seeking  $f$ s yield more robust accuracy improvements and, for these operators, better posterior approximations translate to better task performance.

## Impact Statements

This paper presents work aimed at advancing the field of machine learning by combining language models. There are many potential societal consequences of our work, none of which we feel need to be highlighted here.

## References

- Marah Abdin, Jyoti Aneja, Harkirat Behl, Sébastien Bubeck, Ronen Eldan, Suriya Gunasekar, Michael Harrison, Russell J. Hewett, Mojan Javaheripi, Piero Kauffmann, James R. Lee, Yin Tat Lee, Yuezhi Li, Weishung Liu, Caio C. T. Mendes, Anh Nguyen, Eric Price, Gustavo de Rosa, Olli Saarikivi, Adil Salim, Shital Shah, Xin Wang, Rachel Ward, Yue Wu, Dingli Yu, Cyril Zhang, and Yi Zhang. 2024. *Phi-4 technical report*. *Preprint*, arXiv:2412.08905.
- Shun-ichi Amari. 1985. *Differential-Geometrical Methods in Statistics*, volume 28 of *Lecture Notes in Statistics*. Springer-Verlag.
- Christophe Andrieu and Gareth O. Roberts. 2009. The pseudo-marginal approach for efficient Monte Carlo computations. *arXiv: Statistics Theory*.
- Stephen Boyd and Lieven Vandenbergh. 2004. *Convex Optimization*. Cambridge University Press.
- Sourav Chatterjee and Persi Diaconis. 2018. The sample size required in importance sampling. *The Annals of Applied Probability*, 28.
- Zhijun Chen, Jingzheng Li, Pengpeng Chen, Zhuoran Li, Kai Sun, Yuankai Luo, Qianren Mao, Ming Li, Likang Xiao, Dingqi Yang, Yikun Ban, Hailong Sun, and Philip S. Yu. 2025. Harnessing multiple large language models: A survey on LLM ensemble. *Preprint*, arXiv:2502.18036.
- Jasper Dekoninck, Marc Fischer, Luca Beurer-Kellner, and Martin Vechev. 2024. Controlled text generation via language model arithmetic. In *International Conference on Learning Representations*.
- Pierre Del Moral, Arnaud Doucet, and Ajay Jasra. 2006. Sequential Monte Carlo samplers. *Journal of the Royal Statistical Society: Series B (Statistical Methodology)*, 68(3).
- Juan Luis Gastaldi, John Terilla, Luca Malagutti, Brian DuSell, Tim Vieira, and Ryan Cotterell. 2025. The foundations of tokenization: Statistical and computational concerns. In *International Conference on Learning Representations*.
- Saibo Geng, Hudson Cooper, Michał Moskal, Samuel Jenkins, Julian Berman, Nathan Ranchin, Robert West, Eric Horvitz, and Harsha Nori. 2025. JSONSchemaBench: A rigorous benchmark of structured outputs for language models. *Preprint*, arXiv:2501.10868.
- John Geweke. 1989. Bayesian inference in econometric models using Monte Carlo integration. *Econometrica*, 57(6).
- GlaiveAI. 2024. Glaive function calling dataset. Accessed: 2026-01-22.
- Neha Gupta, Harikrishna Narasimhan, Wittawat Jitkrittum, Ankit Singh Rawat, Aditya Krishna Menon, and Sanjiv Kumar. 2024. Language model cascades: Token-Level uncertainty and beyond. In *International Conference on Learning Representations*.
- Geoffrey E. Hinton. 1999. Products of experts. In *Proceedings of the International Conference on Artificial Neural Networks*, volume 1. Institution of Electrical Engineers.
- Geoffrey E. Hinton. 2002. Training products of experts by minimizing contrastive divergence. *Neural Computing*, 14(8).
- Yichong Huang, Xiaocheng Feng, Baohang Li, Yang Xiang, Hui Wang, Ting Liu, and Bing Qin. 2024. Ensemble learning for heterogeneous large language models with deep parallel collaboration. In *Conference on Neural Information Processing Systems*.
- Dongfu Jiang, Xiang Ren, and Bill Yuchen Lin. 2023. LLM-Blender: Ensembling large language models with pairwise ranking and generative fusion. In *Proceedings of the Annual Meeting of the Association for Computational Linguistics*.
- Lifeng Jin, Baolin Peng, Linfeng Song, Haitao Mi, Ye Tian, and Dong Yu. 2024. Collaborative decoding of critical tokens for boosting factuality of large language models. *Preprint*, arXiv:2402.17982.
- Wittawat Jitkrittum, Neha Gupta, Aditya Krishna Menon, Harikrishna Narasimhan, Ankit Singh Rawat, and Sanjiv Kumar. 2023. When does confidence-based cascade deferral suffice? In *Conference on Neural Information Processing Systems*.
- Michael I. Jordan and Robert A. Jacobs. 1994. Hierarchical mixtures of experts and the EM algorithm. *Neural Computing*, 6(2).
- Muhammad Khalifa, Lajanugen Logeswaran, Moontae Lee, Honglak Lee, and Lu Wang. 2023. Exploring demonstration ensembling for in-context learning. In *ICLR 2023 Workshop on Mathematical and Empirical Understanding of Foundation Models*.

- J. Kittler, M. Hatef, R.P.W. Duin, and J. Matas. 1998. On combining classifiers. *IEEE Transactions on Pattern Analysis and Machine Intelligence*, 20(3).
- Alexander K. Lew, Tan Zhi-Xuan, Gabriel Grand, and Vikash Mansinghka. 2023. Sequential Monte Carlo steering of large language models using probabilistic programs. In *ICML Workshop: Sampling and Optimization in Discrete Space*.
- Tianlin Li, Qian Liu, Tianyu Pang, Chao Du, Qing Guo, Yang Liu, and Min Lin. 2024. Purifying large language models by ensembling a small language model. *Preprint*, arXiv:2402.14845.
- Xiang Lisa Li, Ari Holtzman, Daniel Fried, Percy Liang, Jason Eisner, Tatsunori Hashimoto, Luke Zettlemoyer, and Mike Lewis. 2023. Contrastive decoding: Open-ended text generation as optimization. In *Proceedings of the Annual Meeting of the Association for Computational Linguistics*.
- Hunter Lightman, Vineet Kosaraju, Yuri Burda, Harrison Edwards, Bowen Baker, Teddy Lee, Jan Leike, John Schulman, Ilya Sutskever, and Karl Cobbe. 2024. Let’s verify step by step. In *International Conference on Learning Representations*.
- Ben Lipkin, Benjamin LeBrun, Jacob Hoover Vigly, João Loula, David R. MacIver, Li Du, Jason Eisner, Ryan Cotterell, Vikash Mansinghka, Timothy J. O’Donnell, Alexander K. Lew, and Tim Vieira. 2025. Fast controlled generation from language models with adaptive weighted rejection sampling. In *Conference on Language Modeling*.
- Alisa Liu, Maarten Sap, Ximing Lu, Swabha Swayamdipta, Chandra Bhagavatula, Noah A. Smith, and Yejin Choi. 2021. DExperts: Decoding-time controlled text generation with experts and anti-experts. In *Proceedings of the Annual Meeting of the Association for Computational Linguistics and the 11th International Joint Conference on Natural Language Processing (Volume 1: Long Papers)*.
- Cong Liu, Xiaojun Quan, Yan Pan, Liang Lin, Weigang Wu, and Xu Chen. 2024. Cool-Fusion: Fuse large language models without training. *Preprint*, arXiv:2407.19807.
- Llama Team. 2024. The Llama 3 herd of models. *Preprint*, arXiv:2407.21783.
- João Loula, Benjamin LeBrun, Li Du, Ben Lipkin, Clemente Pasti, Gabriel Grand, Tianyu Liu, Yahya Emara, Marjorie Freedman, Jason Eisner, Ryan Cotterell, Vikash Mansinghka, Alexander K. Lew, Tim Vieira, and Timothy J. O’Donnell. 2025. Syntactic and semantic control of large language models via sequential Monte Carlo. In *International Conference on Learning Representations*.
- Keming Lu, Hongyi Yuan, Runji Lin, Junyang Lin, Zheng Yuan, Chang Zhou, and Jingren Zhou. 2024. Routing to the expert: Efficient reward-guided ensemble of large language models. In *Proceedings of the Conference of the North American Chapter of the Association for Computational Linguistics: Human Language Technologies*.
- Costas Mavromatis, Petros Karypis, and George Karypis. 2024. Pack of LLMs: Model fusion at test-time via perplexity optimization. In *Conference on Language Modeling*.
- Ning Miao, Hao Zhou, Lili Mou, Rui Yan, and Lei Li. 2019. CGMH: Constrained sentence generation by Metropolis-Hastings sampling. *Proceedings of the AAAI Conference on Artificial Intelligence*, 33.
- Art B. Owen. 2013. *Monte Carlo theory, methods and examples*, chapter 9. <https://artowen.su.domains/mc/>. Accessed: 2025-03-15.
- Kanghee Park, Jiayu Wang, Taylor Berg-Kirkpatrick, Nadia Polikarpova, and Loris D’Antoni. 2024. Grammar-aligned decoding. In *Conference on Neural Information Processing Systems*.
- Buu Phan, Brandon Amos, Itai Gat, Marton Havasi, Matthew J. Muckley, and Karen Ullrich. 2025. Exact byte-level probabilities from tokenized language models for FIM-tasks and model ensembles. In *International Conference on Learning Representations*.
- Buu Phan, Ashish J Khisti, and Karen Ullrich. 2026. Cross-tokenizer likelihood scoring algorithms for language model distillation. In *International Conference on Learning Representations*.
- Gabriel Poesia, Alex Polozov, Vu Le, Ashish Tiwari, Gustavo Soares, Christopher Meek, and Sumit Gulwani. 2022. Synchromesh: Reliable code generation from pre-trained language models. In *International Conference on Learning Representations*.
- Felipe Maia Polo, Ronald Xu, Lucas Weber, Mírian Silva, Onkar Bhardwaj, Leshem Choshen, Allysson Flavio Melo de Oliveira, Yuekai Sun, and Mikhail Yurochkin. 2024. Efficient multi-prompt evaluation of LLMs. In *Conference on Neural Information Processing Systems*.
- Lianhui Qin, Sean Welleck, Daniel Khachabi, and Yejin Choi. 2022. COLD decoding: Energy-based constrained text generation with langevin dynamics. In *Conference on Neural Information Processing Systems*.
- Alec Radford, Jeffrey Wu, Rewon Child, David Luan, Dario Amodei, Ilya Sutskever, et al. 2019. Language models are unsupervised multitask learners. *OpenAI blog*, 1(8).

- Christian P. Robert and George Casella. 2005. *Monte Carlo Statistical Methods*. Springer-Verlag.
- Sheldon M. Ross. 2023. *Additional variance reduction techniques*. In *Simulation*, sixth edition. Academic Press.
- Tal Shnitzer, Anthony Ou, Mírian Silva, Kate Soule, Yuekai Sun, Justin Solomon, Neil Thompson, and Mikhail Yurochkin. 2024. *Large language model routing with benchmark datasets*. In *Conference on Language Modeling*.
- Ruoxi Sun, Sercan Arik, Rajarishi Sinha, Hootan Nakhost, Hanjun Dai, Pengcheng Yin, and Tomas Pfister. 2023. *SQLPrompt: In-context text-to-SQL with minimal labeled data*. In *Findings of the Association for Computational Linguistics: EMNLP 2023*.
- Mirac Suzgun, Nathan Scales, Nathanael Schärli, Sebastian Gehrmann, Yi Tay, Hyung Won Chung, Aakanksha Chowdhery, Quoc Le, Ed Chi, Denny Zhou, and Jason Wei. 2023. *Challenging BIG-bench tasks and whether chain-of-thought can solve them*. In *Findings of the Association for Computational Linguistics: ACL 2023*.
- Tim Vieira, Benjamin LeBrun, Mario Giulianelli, Juan Luis Gastaldi, Brian DuSell, John Terilla, Timothy J. O’Donnell, and Ryan Cotterell. 2025a. *From language models over tokens to language models over characters*. In *International Conference on Machine Learning*.
- Tim Vieira, Tianyu Liu, Clemente Pasti, Yahya Emara, Brian DuSell, Benjamin LeBrun, Mario Giulianelli, Juan Luis Gastaldi, John Terilla, Timothy J. O’Donnell, and Ryan Cotterell. 2025b. *Language models over canonical byte-pair encodings*. In *International Conference on Machine Learning*.
- Yangyifan Xu, Jinliang Lu, and Jiajun Zhang. 2024. *Bridging the gap between different vocabularies for LLM ensemble*. In *Proceedings of the Conference of the North American Chapter of the Association for Computational Linguistics: Human Language Technologies*.
- An Yang, Baosong Yang, Beichen Zhang, Binyuan Hui, Bo Zheng, Bowen Yu, Chengyuan Li, Dayiheng Liu, Fei Huang, Haoran Wei, Huan Lin, Jian Yang, Jianhong Tu, Jianwei Zhang, Jianxin Yang, Jiayi Yang, Jingren Zhou, Junyang Lin, Kai Dang, Keming Lu, Keqin Bao, Kexin Yang, Le Yu, Mei Li, Mingfeng Xue, Pei Zhang, Qin Zhu, Rui Men, Runji Lin, Tianhao Li, Tianyi Tang, Tingyu Xia, Xingzhang Ren, Xuancheng Ren, Yang Fan, Yang Su, Yichang Zhang, Yu Wan, Yuqiong Liu, Zeyu Cui, Zhenru Zhang, and Zihan Qiu. 2025. *Qwen2.5 technical report*. Preprint, arXiv:2412.15115.
- Yuxuan Yao, Han Wu, Mingyang LIU, Sichun Luo, Xiongwei Han, Jie Liu, Zhijiang Guo, and Linqi Song. 2025. *Determine-then-ensemble: Necessity of top-k union for large language model ensembling*. In *International Conference on Learning Representations*.
- Tao Yu, Rui Zhang, Kai Yang, Michihiro Yasunaga, Dongxu Wang, Zifan Li, James Ma, Irene Li, Qingning Yao, Shanelle Roman, Zilin Zhang, and Dragomir Radev. 2018. *Spider: A large-scale human-labeled dataset for complex and cross-domain semantic parsing and text-to-SQL task*. In *Proceedings of the Conference on Empirical Methods in Natural Language Processing*.
- Yao-Ching Yu, Chun Chih Kuo, Ye Ziqi, Chang Yucheng, and Yueh-Se Li. 2024. *Breaking the ceiling of the LLM community by treating token generation as a classification for ensembling*. In *Findings of the Association for Computational Linguistics: EMNLP 2024*.
- Maosen Zhang, Nan Jiang, Lei Li, and Yexiang Xue. 2020. *Language generation via combinatorial constraint satisfaction: A tree search enhanced Monte-Carlo approach*. In *Findings of the Association for Computational Linguistics: EMNLP 2020*.
- Stephen Zhao, Rob Brekelmans, Alireza Makhzani, and Roger Baker Grosse. 2024. *Probabilistic inference in language models via twisted sequential Monte Carlo*. In *International Conference on Machine Learning*.

## A. Related Work

**Ensembling Language Models.** A recent survey by Chen et al. (2025) taxonomizes recent work around language model ensembling. Namely, they categorize these works into three major groups based on the stage where ensembling occurs: *before*, *during*, and *after* decoding. Methods applied *before* decoding typically involve routing queries to specific models based on predicted performance or cost, such as the classification-based routing by Shnitzer et al. (2024) or reward-guided methods like Zooter (Lu et al., 2024). Conversely, *after* decoding approaches focus on selecting or fusing complete responses generated by multiple models; prominent examples include pairwise ranking in LLM-Blender (Jiang et al., 2023), best-of- $N$  sampling (Lightman et al., 2024), or cascade systems (Jitkrittum et al., 2023; Gupta et al., 2024). Finally, ensembling *during* decoding involves aggregating predictions at the token or span level to guide generation, which is the subject of this study.

**Ensembling Language Models During Sampling.** Existing methods for combining language models at the token level often grapple with the vocabulary alignment problem: incompatible tokenizers yield distributions over mismatching vocabularies. To address this, recent works have proposed mapping distributions into a shared space to enable probability aggregation. For instance, Yu et al. (2024) introduce a union vocabulary approach, projecting distributions onto a superset of tokens from all participating models, then computing the average token probability across models. Yao et al. (2025) refine this by constructing a union over only the top- $k$  tokens, thereby reducing computational overhead while maintaining alignment. Alternatively, approaches like DeePen (Huang et al., 2024) and EVA (Xu et al., 2024) bypass explicit vocabulary unification by projecting outputs into a shared relative embedding space or using pivot mechanisms to fuse distributions. Other techniques, such as PackLLM (Mavromatis et al., 2024), focus on dynamic weighting, adjusting the influence of each model based on step-wise perplexity. Most relatedly, Phan et al. (2025) implements an experiment for combining byte-level language models of different model families via probability averaging. Crucially, the main focus of many of these papers lies in developing heuristics for dealing with the vocabulary alignment problem, while applying averages (Yu et al., 2024; Xu et al., 2024; Yao et al., 2025) or some type of weighted averages (Huang et al., 2024; Mavromatis et al., 2024; Jin et al., 2024; Li et al., 2024) to the token probabilities.

In our work, we leverage prior methods for mapping language models to a shared character vocabulary (Phan et al., 2025; Vieira et al., 2025a), which sidesteps the alignment problem entirely. This allows us to focus on a different question: in what other ways can language model distributions be combined? We explore alternatives to probability averaging and propose an SMC-based ensembling algorithm that enables, in the limit, consistent sampling from the combined distribution.

**Approximate Posterior Inference for Large Language Models During Sampling.** A growing line of work formulates constrained generation from language models as posterior inference, employing approximate inference algorithms to sample from intractable target distributions. Several approaches have been explored, including rejection sampling (Poesia et al., 2022; Lipkin et al., 2025), MCMC methods (Miao et al., 2019; Zhang et al., 2020; Qin et al., 2022), and sequential Monte Carlo (Lew et al., 2023; Zhao et al., 2024; Loula et al., 2025). Of these, SMC is particularly well-suited to language models as it exploits autoregressive factorization, avoiding the need to re-evaluate entire sequences after each modification. Lew et al. (2023) introduced SMC steering of LMs via probabilistic programs, enabling globally consistent sampling from conditional targets while only computing local constraints. Zhao et al. (2024) developed learned twist functions via contrastive training to guide SMC toward high-value completions, along with bidirectional bounds on the log-partition function for evaluating inference quality. Most recently, Loula et al. (2025) applied SMC to sample from the global product of a language model and various syntactic and semantic potentials, demonstrating improved performance from better posterior approximations.

These prior works focus on combining a *single* language model with external constraints (e.g., grammars, semantic specifications). In contrast, we study the composition of *multiple* language models via general aggregation functions  $f$ , where the target distribution arises from the models themselves rather than auxiliary constraints. This setting introduces distinct challenges: the choice of  $f$  induces qualitatively different ensemble behaviors, and we systematically study how both  $f$  and approximation quality affect downstream performance.

## B. Limitations

We acknowledge the following limitations of our paper.

**Computational cost.** Our approach relies on sequential Monte Carlo, which, as noted by Loula et al. (2025), introduces inference-time overhead relative to standard decoding due to maintaining multiple particles and performing resampling. This cost is amplified at the byte level: sequences require more SMC steps, and computing byte-level next-symbol probabilities from tokenized LMs requires marginalizing over admissible tokenizations. However, we note that SMC can operate

in parallel across particles, and recent work on speculative decoding and efficient inference may help mitigate these costs. Moreover, for applications where output quality is important—such as high-stakes decision-making or constrained generation—the improved accuracy from better posterior approximations may justify the additional computation.

**Number of experts.** We focus on ensembling two language models to enable controlled analysis of pairwise interactions between experts and aggregation functions. This design choice allows us to isolate the effects of different  $f$ -ensembles without confounding factors from complex multi-expert dynamics. Our framework naturally extends to  $K > 2$  experts, which may yield further performance gains through increased diversity. We leave systematic study of scaling the number of experts to future work.

**Scope of ensembling.** As discussed in Appendix A, our work focuses on ensembling language models *during* decoding, i.e., combining next-token distributions at each generation step. This is distinct from other inference—time combination strategies. Model routing (Shnitzer et al., 2024) selects a single model per query, avoiding the cost of running multiple models but forgoing the benefits of combining their predictions at the token level. Post-hoc methods like best-of- $N$  (Lightman et al., 2024) or LLM-Blender (Jiang et al., 2023) generate complete outputs from each model and then select or fuse among them, enabling comparison of full sequences but requiring multiple complete generations. Our during-decoding approach intervenes at every token, allowing the ensemble to steer generation toward globally promising regions before committing to a full sequence. These paradigms are complementary: for instance, during-decoding ensembles could be combined with post-hoc reranking for further gains.

**Model selection.** We evaluate instruction-tuned models (Llama, Qwen, Phi) in the 7–14B parameter range. This choice balances experimental tractability with practical relevance; these models are widely deployed and accessible to practitioners. We do not evaluate reasoning-specialized models (e.g., models trained with chain-of-thought or process supervision) or larger frontier models, which may exhibit different ensembling dynamics. Exploring whether consensus-seeking ensembles can combine the strengths of specialized reasoners is a promising direction for future work.

**Task selection.** We evaluate on structured text generation tasks (JSON schema conformance, word sorting, text-to-SQL) with objective, binary correctness criteria. This choice is deliberate: structured tasks allow resampling effects to manifest over multiple generation steps, and objective evaluation enables rigorous comparison of methods. Our findings demonstrate clear benefits from consensus-seeking ensembles and better posterior approximations in this setting. Whether these benefits transfer to open-ended generation tasks (e.g., creative writing, dialogue) remains an open question, as evaluation in such settings is harder to evaluate.

## C. Tokenized Language Models

Modern language models are typically designed as probability distributions over strings of *tokens* rather than over strings of bytes. Although one byte string admits only one tokenization, multiple sequences of tokens may correspond to the same string of bytes. This has two fundamental consequences. First, the LM may spread probability mass among multiple valid tokenizations of a byte string (Phan et al., 2025; Vieira et al., 2025a;b). Second, when comparing the probability that two different models assign to a given string—as we do in the *ensemble* framework—one cannot directly compare token-level probabilities because the models may tokenize the string differently.

To combine such models, we must map them to a common space. As all valid tokenizations of a string ultimately decode to the string itself, one possible way is to consider the probability distribution over byte strings.<sup>14,15</sup> This section formalizes this connection through the notion of a *tokenized language model*. In order to introduce this notion, we define a *tokenization model* (Gastaldi et al., 2025) as a tuple  $\langle \Sigma, \Delta, \tau, \kappa \rangle$ , where  $\Delta$  and  $\Sigma$  are respectively the token and byte alphabet,  $\tau: \Sigma^* \rightarrow \Delta^*$  is the tokenizer, and  $\kappa: \Delta^* \rightarrow \Sigma^*$  is a decoding function that must satisfy  $\kappa(\tau(\mathbf{x})) = \mathbf{x}$ .

**Definition C.1.** Let  $\Delta$  be an alphabet of token symbols,  $\Sigma$  an alphabet of character symbols, and  $p_\Delta$  a language model over  $\Delta^*$ . A *tokenized language model*  $p_\Sigma$  is a language model over  $\Sigma^*$  that is induced by the decoding function  $\kappa: \Delta^* \rightarrow \Sigma^*$ :

$$p_\Sigma(\mathbf{x}) \stackrel{\text{def}}{=} \mathbb{P}_{Y \sim p_\Delta} [\kappa(Y) = \mathbf{x}] \quad (15)$$

Note that  $p_\Sigma(\mathbf{x})$  correctly accounts for the fact that *many* token strings  $Y$  may map to a given character string  $\mathbf{x}$  through the

<sup>14</sup>In practice, we first use a layer for mapping character strings to byte strings  $\mathcal{B}^*$ , where  $\mathcal{B} = \{0, \dots, 255\}$ .

<sup>15</sup>Note that an alternative approach is to map a language model’s distribution to another language model’s tokenization space (Phan et al., 2026).

decoding function  $\kappa$ . The prefix probability  $\vec{p}_\Sigma$  follows automatically from Eqs. (1) and (2).

## D. Deferred Proofs

### D.1. Importance Sampling

**Proposition D.1.** *Importance sampling has the following guarantees:*

1. *The estimated normalization constant is unbiased:*

$$\mathbb{E}_{\mathbf{x}^{(1)}, \dots, \mathbf{x}^{(M)} \stackrel{i.i.d.}{\sim} r} [\widehat{Z}] = Z \quad (16)$$

2. *The estimated target function is unbiased:*

$$\mathbb{E}_{\mathbf{x}^{(1)}, \dots, \mathbf{x}^{(M)} \stackrel{i.i.d.}{\sim} r} [\widehat{\varphi}(\mathbf{x})] = \varphi(\mathbf{x}) \quad (17)$$

3. *The estimated distribution is consistent:*

$$\lim_{M \rightarrow \infty} \mathbb{E}_{\mathbf{x}^{(1)}, \dots, \mathbf{x}^{(M)} \stackrel{i.i.d.}{\sim} r} [\widehat{\Phi}(\mathbf{x})] = \Phi(\mathbf{x}) \quad (18)$$

*Proof. Part (1).* The fact that  $\widehat{Z}$  is an unbiased estimator of  $Z$  follows from the definition of  $\mathbb{E}$  and its linearity under the assumption that  $r(\mathbf{x}) = 0 \implies \varphi(\mathbf{x}) = 0$  for all  $\mathbf{x} \in \Sigma^*$  (e.g., Ross, 2023):

$$\mathbb{E}_{\mathbf{x}^{(1)}, \dots, \mathbf{x}^{(M)} \stackrel{i.i.d.}{\sim} r} [\widehat{Z}] = \mathbb{E}_{\mathbf{x}^{(1)}, \dots, \mathbf{x}^{(M)} \stackrel{i.i.d.}{\sim} r} \left[ \frac{1}{M} \sum_{m=1}^M w^{(m)} \right] \quad [\text{Def. 5.1}] \quad (19a)$$

$$= \frac{1}{M} \sum_{m=1}^M \mathbb{E}_{\mathbf{x}^{(m)} \stackrel{i.i.d.}{\sim} r} [w^{(m)}] \quad [\text{Independence}] \quad (19b)$$

$$= \frac{1}{M} \sum_{m=1}^M \mathbb{E}_{\mathbf{x} \sim r} \left[ \frac{\varphi(\mathbf{x})}{r(\mathbf{x})} \right] \quad [\text{Identity}] \quad (19c)$$

$$= \mathbb{E}_{\mathbf{x} \sim r} \left[ \frac{\varphi(\mathbf{x})}{r(\mathbf{x})} \right] \quad [\text{Algebra}] \quad (19d)$$

$$= \sum_{\mathbf{x} \in \Sigma^*} r(\mathbf{x}) \frac{\varphi(\mathbf{x})}{r(\mathbf{x})} \quad [\text{Def. of } \mathbb{E}] \quad (19e)$$

$$= \sum_{\mathbf{x} \in \Sigma^*} \varphi(\mathbf{x}) \quad [\text{Algebra, Absolute Continuity}] \quad (19f)$$

$$= Z \quad (19g)$$

**Part (2).** Under the same assumptions as above, we similarly show that  $\widehat{\varphi}$  is an unbiased estimator of  $\varphi$ . Choose  $\mathbf{x} \in \Sigma^*$

arbitrarily.

$$\mathbb{E}_{\mathbf{x}^{(1)}, \dots, \mathbf{x}^{(M)} \stackrel{\text{i.i.d.}}{\sim} r} [\widehat{\varphi}(\mathbf{x})] = \mathbb{E}_{\mathbf{x}^{(1)}, \dots, \mathbf{x}^{(M)} \stackrel{\text{i.i.d.}}{\sim} r} \left[ \frac{1}{M} \sum_{m=1}^M w^{(m)} \mathbb{1}\{\mathbf{x} = \mathbf{x}^{(m)}\} \right] \quad [\text{Eq. (8)}] \quad (20a)$$

$$= \frac{1}{M} \sum_{m=1}^M \mathbb{E}_{\mathbf{x}^{(m)} \stackrel{\text{i.i.d.}}{\sim} r} w^{(m)} \mathbb{1}\{\mathbf{x} = \mathbf{x}^{(m)}\} \quad [\text{Independence}] \quad (20b)$$

$$= \mathbb{E}_{\mathbf{x}' \sim r} \left[ \frac{\varphi(\mathbf{x}')}{r(\mathbf{x}')} \mathbb{1}\{\mathbf{x} = \mathbf{x}'\} \right] \quad [\text{Definition of importance weight}] \quad (20c)$$

$$= \sum_{\mathbf{x}' \in \Sigma^*} r(\mathbf{x}') \frac{\varphi(\mathbf{x}')}{r(\mathbf{x}')} \mathbb{1}\{\mathbf{x} = \mathbf{x}'\} \quad [\text{Def. of } \mathbb{E}] \quad (20d)$$

$$= \sum_{\mathbf{x}' \in \Sigma^*} \varphi(\mathbf{x}') \mathbb{1}\{\mathbf{x} = \mathbf{x}'\} \quad [\text{Algebra, Absolute Continuity}] \quad (20e)$$

$$= \varphi(\mathbf{x}) \quad (20f)$$

**Part (3).** Pick  $\mathbf{x} \in \Sigma^*$  arbitrarily, then consistency of the estimator follows under mild assumptions, the strong law of large numbers (SLLN) (e.g., Geweke, 1989; Owen, 2013), gives us the following

$$\lim_{M \rightarrow \infty} \mathbb{E}_{\mathbf{x}^{(1)}, \dots, \mathbf{x}^{(M)} \stackrel{\text{i.i.d.}}{\sim} r} [\widehat{\Phi}(\mathbf{x})] = \lim_{M \rightarrow \infty} \mathbb{E}_{\mathbf{x}^{(1)}, \dots, \mathbf{x}^{(M)} \stackrel{\text{i.i.d.}}{\sim} r} \left[ \frac{\frac{1}{M} \sum_{m=1}^M w^{(m)} \mathbb{1}\{\mathbf{x} = \mathbf{x}^{(m)}\}}{\frac{1}{M} \sum_{m=1}^M w^{(m)}} \right] \quad [\text{Def. 5.1}] \quad (21a)$$

$$= \frac{\mathbb{E}_{\mathbf{x}' \sim r} \left[ \frac{\varphi(\mathbf{x}')}{r(\mathbf{x}')} \mathbb{1}\{\mathbf{x} = \mathbf{x}'\} \right]}{\mathbb{E}_{\mathbf{x}' \sim r} \left[ \frac{\varphi(\mathbf{x}')}{r(\mathbf{x}')} \right]} \quad [\text{a.s. under SLLN}] \quad (21b)$$

$$= \frac{\varphi(\mathbf{x})}{Z} \quad [\widehat{Z}, \widehat{\varphi} \text{ unbiased}] \quad (21c)$$

$$= \Phi(\mathbf{x}) \quad [\text{Def. 4.1}] \quad (21d)$$

■

**Proposition 5.2.** *The locally optimal proposal distribution i.e., the one that minimizes the variance of the importance weight update at each step, is  $\vec{r}^*(x' | \mathbf{x}) \propto \vec{\psi}(x' | \mathbf{x})$ .*

*Proof.* Suppose we fix a given string  $\mathbf{x}$ , and we wanted to choose the proposal distribution  $\vec{r}(\cdot | \mathbf{x})$  to minimize the variance of the importance weight

$$w(x', \mathbf{x}) \stackrel{\text{def}}{=} \frac{\vec{\psi}(x' | \mathbf{x})}{\vec{r}(x' | \mathbf{x})} \quad (22)$$

The expected value of the importance weight is

$$\mathbb{E}_{x' \sim \vec{r}(\cdot | \mathbf{x})} \left[ \frac{\vec{\psi}(x' | \mathbf{x})}{\vec{r}(x' | \mathbf{x})} \right] = \sum_{x' \in \Sigma} \vec{r}(x' | \mathbf{x}) \frac{\vec{\psi}(x' | \mathbf{x})}{\vec{r}(x' | \mathbf{x})} = \sum_{x' \in \Sigma} \vec{\psi}(x' | \mathbf{x}) \quad (23a)$$

Thus, the variance of the weight is

$$\text{Var}(w(x', \mathbf{x}))_{x' \sim \vec{r}(\cdot | \mathbf{x})} = \mathbb{E}_{x' \sim \vec{r}(\cdot | \mathbf{x})} [w(x', \mathbf{x})^2] - \left( \sum_{x' \in \Sigma} \vec{\psi}(x' | \mathbf{x}) \right)^2 \quad (24a)$$

$$= - \left( \sum_{x' \in \Sigma} \vec{\psi}(x' | \mathbf{x}) \right)^2 + \sum_{x' \in \Sigma} \vec{r}(x' | \mathbf{x}) \frac{\vec{\psi}(x' | \mathbf{x})^2}{\vec{r}(x' | \mathbf{x})^2} \quad (24b)$$

$$= - \left( \sum_{x' \in \Sigma} \vec{\psi}(x' | \mathbf{x}) \right)^2 + \sum_{x' \in \Sigma} \frac{\vec{\psi}(x' | \mathbf{x})^2}{\vec{r}(x' | \mathbf{x})} \quad (24c)$$

Our goal is to minimize Eq. (24a) under the *constraints* that the proposal should be a valid probability distribution over tokens, i.e.,  $\vec{r}(x' | \mathbf{x}) \geq 0$  for all  $x'$  and  $\sum_{x' \in \Sigma} \vec{r}(x' | \mathbf{x}) = 1$ . We can formulate this problem using the method of Lagrange multipliers, i.e.,

$$L = - \left( \sum_{x' \in \Sigma} \vec{\psi}(x' | \mathbf{x}) \right)^2 + \sum_{x' \in \Sigma} \frac{\vec{\psi}(x' | \mathbf{x})^2}{\vec{r}(x' | \mathbf{x})} - \lambda \left( 1 - \sum_{x' \in \Sigma} \vec{r}(x' | \mathbf{x}) \right) \quad (25)$$

as a function of the Lagrange multiplier  $\lambda$ . Then,

$$\frac{\partial}{\partial \vec{r}(x'' | \mathbf{x})} L = \sum_{x' \in \Sigma} \frac{\partial}{\partial \vec{r}(x'' | \mathbf{x})} \frac{\vec{\psi}(x' | \mathbf{x})^2}{\vec{r}(x' | \mathbf{x})} + \lambda \sum_{x' \in \Sigma} \frac{\partial}{\partial \vec{r}(x'' | \mathbf{x})} \vec{r}(x' | \mathbf{x}) \quad (26a)$$

$$= \sum_{x' \in \Sigma} - \frac{\vec{\psi}(x' | \mathbf{x})^2}{\vec{r}(x' | \mathbf{x})^2} \mathbb{1}\{x' = x''\} + \lambda \sum_{x' \in \Sigma} \mathbb{1}\{x' = x''\} \quad (26b)$$

$$= - \frac{\vec{\psi}(x'' | \mathbf{x})^2}{\vec{r}(x'' | \mathbf{x})^2} + \lambda \quad (26c)$$

Solving for  $\frac{\partial L}{\partial \vec{r}(x'' | \mathbf{x})} = 0$  gives

$$0 = - \frac{\vec{\psi}(x'' | \mathbf{x})^2}{\vec{r}(x'' | \mathbf{x})^2} + \lambda \quad (27a)$$

$$\vec{r}(x'' | \mathbf{x})^2 = \frac{\vec{\psi}(x'' | \mathbf{x})^2}{\lambda} \quad (27b)$$

$$\vec{r}(x'' | \mathbf{x}) = \pm \sqrt{\frac{\vec{\psi}(x'' | \mathbf{x})^2}{\lambda}} \quad (27c)$$

As  $\vec{r}(x' | \mathbf{x}) \geq 0$ , the only valid solution is  $\vec{r}^*(x' | \mathbf{x}) = \frac{\vec{\psi}(x' | \mathbf{x})}{\sqrt{\lambda}}$ . Substituting the optimal choice into  $\vec{r}(x' | \mathbf{x})$  into the constraint  $\sum_{x' \in \Sigma} \vec{r}(x' | \mathbf{x}) = 1$  and solving for the value of  $\sqrt{\lambda}$  that makes it hold

$$1 = \sum_{x'' \in \Sigma} \vec{r}^*(x'' | \mathbf{x}) \quad (28a)$$

$$= \sum_{x'' \in \Sigma} \frac{\vec{\psi}(x'' | \mathbf{x})}{\sqrt{\lambda}} \quad (28b)$$

$$\sqrt{\lambda} = \sum_{x'' \in \Sigma} \vec{\psi}(x'' | \mathbf{x}) \quad (28c)$$

Thus, the optimal choice for  $\vec{r}(\cdot | \mathbf{x})$  is  $\vec{r}^*(x'' | \mathbf{x}) \propto \vec{\psi}(x'' | \mathbf{x})$ . In the context of the Karush-Kuhn-Tucker conditions, the nonnegativity constraints are inactive at the optimum (since all components of  $\vec{r}^*$  are strictly positive), which justifies why the Lagrangian can be formulated using only the equality constraint. We also note that this is a convex quadratic subject to linear constraints; thus, the solution is globally optimal (Chapter 4; Boyd and Vandenberghe, 2004). ■

## D.2. Absolute Continuity and $f$

The discussion of absolute continuity raises a practical question: for what  $f$  does our standard choice of shaping function,  $\vec{\psi}(\mathbf{x}) = f(\vec{p}_1(\mathbf{x}), \dots, \vec{p}_K(\mathbf{x}))$ , automatically satisfy this requirement?

**Definition D.1.** For our choice of shaping function (cf. §5.2), the absolute continuity condition  $\vec{\psi}(\mathbf{x}) = 0 \implies \vec{\Phi}(\mathbf{x}) = 0$  imposes for  $f$  to fulfill

$$f(\vec{p}_1(\mathbf{x}'), \dots, \vec{p}_K(\mathbf{x}')) = 0 \implies f(p_1(\mathbf{x}), \dots, p_K(\mathbf{x})) = 0 \quad (29)$$

for any prefix  $\mathbf{x}'$  of  $\mathbf{x}$ . We call such a set of functions **annihilative**—that is, if any prefix of a string is mapped to zero, then the entire string must also be mapped to zero.

We note that when  $f$  does not satisfy annihilativity<sup>16</sup>; this simply means that the standard shaping function  $\vec{\psi}(\mathbf{x}) = f(\vec{p}_1(\mathbf{x}), \dots, p_K(\mathbf{x}))$  is not a suitable choice. However, simple modifications to our choice of  $\vec{\psi}(\mathbf{x})$  can recover absolute continuity. For instance, setting  $\vec{\psi}(\mathbf{x}) = |f(\vec{p}_1(\mathbf{x}'), \dots, \vec{p}_K(\mathbf{x}'))| + \epsilon$  for  $\epsilon > 0$  may increase the variance of the importance weights, but ensures  $\vec{\psi}(\mathbf{x}) > 0$  for all  $\mathbf{x} \in \Sigma^*$ .

## D.3. Alpha-Divergence Ensembles

**Theorem 4.1** ( $\alpha$ -Divergence Ensembles). Let  $D_\alpha$  be the  $\alpha$ -divergence with parameter  $\alpha \in \mathbb{R} \setminus \{0, 1\}$ . The unique consensus distribution  $\Phi^*$  that minimizes the expert-weighted loss in Eq. (4) is the **generalized mean** of the experts, with power parameter  $\tau \stackrel{\text{def}}{=} 1 - \alpha$ :

$$\Phi^*(\mathbf{x}) = \frac{1}{Z} \left( \sum_{k=1}^K w_k p_k(\mathbf{x})^\tau \right)^{\frac{1}{\tau}} \quad (6)$$

where  $Z$  is the normalizer ensuring  $\sum_{\mathbf{x} \in \Sigma^*} \Phi^*(\mathbf{x}) = 1$ .

*Proof.* To find the optimal consensus distribution  $\Phi^*$ , we minimize the expert-weighted sum of  $\alpha$ -divergences subject to the constraint that  $\Phi$  lies on the simplex (i.e.,  $\sum_{\mathbf{x} \in \mathcal{X}} \Phi(\mathbf{x}) = 1$ ). We formulate the Lagrangian  $\Lambda$ :

$$\begin{aligned} \Lambda(\Phi, \nu) &= \sum_{k=1}^K \frac{w_k}{\alpha(1-\alpha)} \left( 1 - \sum_{\mathbf{x} \in \mathcal{X}} \Phi(\mathbf{x})^\alpha p_k(\mathbf{x})^{1-\alpha} \right) \\ &\quad + \nu \left( \sum_{\mathbf{x} \in \mathcal{X}} \Phi(\mathbf{x}) - 1 \right). \end{aligned} \quad (30)$$

We take the partial derivative with respect to  $\Phi(\mathbf{x})$  for a specific element  $\mathbf{x} \in \mathcal{X}$ :

$$\begin{aligned} \frac{\partial \Lambda}{\partial \Phi(\mathbf{x})} &= - \sum_{k=1}^K \frac{w_k}{\alpha(1-\alpha)} \cdot \alpha \Phi(\mathbf{x})^{\alpha-1} p_k(\mathbf{x})^{1-\alpha} + \nu \\ &= - \frac{\Phi(\mathbf{x})^{\alpha-1}}{1-\alpha} \sum_{k=1}^K w_k p_k(\mathbf{x})^{1-\alpha} + \nu. \end{aligned} \quad (31)$$

Setting the derivative to zero for stationarity:

$$\nu = \frac{\Phi(\mathbf{x})^{\alpha-1}}{1-\alpha} \sum_{k=1}^K w_k p_k(\mathbf{x})^{1-\alpha}. \quad (32)$$

Rearranging to solve for  $\Phi(\mathbf{x})$ :

$$\Phi(\mathbf{x})^{\alpha-1} = \nu(1-\alpha) \left( \sum_{k=1}^K w_k p_k(\mathbf{x})^{1-\alpha} \right)^{-1}. \quad (33)$$

<sup>16</sup>An example of non-annihilativity is the class of contrastive ensembles, e.g.,  $f(p_1, p_2) = (p_1(\mathbf{x}) - p_2(\mathbf{x}))^2$ , which are sometimes used for language model steering (Li et al., 2023; Dekoninck et al., 2024).

Raising both sides to the power of  $\frac{1}{\alpha-1}$  (equivalently  $-\frac{1}{1-\alpha}$ ):

$$\Phi(\mathbf{x}) \propto \left( \sum_{k=1}^K w_k p_k(\mathbf{x})^{1-\alpha} \right)^{\frac{1}{1-\alpha}}. \quad (34)$$

Finally, enforcing the normalization constraint  $\sum_{\mathbf{x} \in \mathcal{X}} \Phi(\mathbf{x}) = 1$  yields the partition function  $Z$ , recovering the generalized mean form with exponent  $\tau = 1 - \alpha$ . ■

**Proposition D.2.** *The family of generalized means  $M_\tau$  defined in Eq. (6) is annihilative for all  $\tau \in \mathbb{R} \setminus \{0\}$  and the limit cases  $\tau \rightarrow \pm\infty$ , and  $\tau \rightarrow 0$ .*

*Proof.* Let  $p_1(\mathbf{x}), \dots, p_K(\mathbf{x})$  denote the probabilities assigned to string  $\mathbf{x}$  by  $K$  language models, and let  $\mathbf{x}'$  be a prefix of  $\mathbf{x}$ . We denote the prefix probabilities by  $\vec{p}_1(\mathbf{x}'), \dots, \vec{p}_K(\mathbf{x}')$ . We evaluate different domains of  $\tau$ :

1.  $\tau > 0$ . For positive  $\tau$ , we have

$$M_\tau(\vec{p}_1(\mathbf{x}'), \dots, \vec{p}_K(\mathbf{x}')) = \left( \frac{1}{K} \sum_{i=1}^K \vec{p}_i(\mathbf{x}')^\tau \right)^{1/\tau} = 0 \quad (35)$$

if and only if  $\sum_{i=1}^K \vec{p}_i(\mathbf{x}')^\tau = 0$ . Since each term  $\vec{p}_i(\mathbf{x}')^\tau \geq 0$ , this requires  $\vec{p}_i(\mathbf{x}') = 0$  for all  $i \in \{1, \dots, K\}$ . By Eq. (3), this implies  $p_k(\mathbf{x}) = 0$ , which implies

$$M_\tau(p_1(\mathbf{x}), \dots, p_K(\mathbf{x})) = 0. \quad (36)$$

Thus, annihilativity holds.

2.  $\tau \rightarrow 0$ . Taking the limit as  $\tau \rightarrow 0$ , we obtain the geometric mean:

$$M_0(\vec{p}_1(\mathbf{x}'), \dots, \vec{p}_K(\mathbf{x}')) = \left( \prod_{i=1}^K \vec{p}_i(\mathbf{x}') \right)^{1/K} = 0 \quad (37)$$

if and only if  $\vec{p}_i(\mathbf{x}') = 0$  for at least one  $i \in \{1, \dots, K\}$ . By Eq. (3), if  $\vec{p}_i(\mathbf{x}') = 0$ , then  $p_i(\mathbf{x}) = 0$ , which implies

$$M_0(p_1(\mathbf{x}), \dots, p_K(\mathbf{x})) = \left( \prod_{j=1}^K p_j(\mathbf{x}) \right)^{1/K} = 0. \quad (38)$$

Thus, annihilativity holds.

3.  $\tau < 0$ . For negative  $\tau$ , the generalized mean is defined by continuity: if any  $\vec{p}_i(\mathbf{x}') = 0$ , we set  $M_\tau = 0$ . If  $M_\tau(\vec{p}_1(\mathbf{x}'), \dots, \vec{p}_K(\mathbf{x}')) = 0$ , then at least one  $\vec{p}_i(\mathbf{x}') = 0$ . By Eq. (3),  $p_i(\mathbf{x}) = 0$ , which implies

$$M_\tau(p_1(\mathbf{x}), \dots, p_K(\mathbf{x})) = 0. \quad (39)$$

Thus, annihilativity holds.

4.  $\tau \rightarrow \pm\infty$ . In the limit  $\tau \rightarrow -\infty$ , we obtain  $M_{-\infty} = \min_i \vec{p}_i(\mathbf{x}')$ , which equals zero if and only if at least one  $\vec{p}_i(\mathbf{x}') = 0$ . In the limit  $\tau \rightarrow +\infty$ , we obtain  $M_{+\infty} = \max_i \vec{p}_i(\mathbf{x}')$ , which equals zero if and only if all  $\vec{p}_i(\mathbf{x}') = 0$ . In both cases, by Eq. (3), the corresponding  $p_i(\mathbf{x}) = 0$ , which implies  $M_{\pm\infty}(p_1(\mathbf{x}), \dots, p_K(\mathbf{x})) = 0$ . Thus, annihilativity holds. ■

## E. Experimental Details

We served models on two 24GB RTX 4090 GPUs and ran the SMC loop on one 24GB RTX 3090 GPU, where the generated predictions were aggregated. We used vLLM<sup>17</sup> for serving all models. The models are loaded in bfloat16 data type. The sampling temperature is set to 1.0.

<sup>17</sup><https://docs.vllm.ai/en/>

**Runtime analysis.** In Table 3, we show per sample, averaged runtimes for token-level, as well as byte-level SMC, and compare it to running inference on a single base model, and doing standard locally normalized ensembling. Local ensembling incurs approximately 3-4x overhead over base model inference, reflecting the cost of running two forward passes. Token-level SMC with  $M = 10$  particles requires 15-24 seconds per instance, roughly 6-7x slower than local ensembling, with runtime scaling approximately linearly in  $M$ . Byte-level SMC is substantially more expensive, requiring 47-167 seconds per instance at  $M = 10$ , comparable to token-level SMC with  $M = 75$ . This increased cost reflects the longer sequence lengths at the byte level: each token expands to multiple bytes, proportionally increasing the number of SMC steps and the number of model calls required to score each particle. A way to improve runtimes is to enhance batching or optimize pruning in our byte-level language model.

Table 3. Average per-instance runtime (seconds) on JSON. Token SMC and Byte SMC use  $M$  particles.

Model	Base Model	Local Ensemble	Token SMC			Byte SMC
			$M=10$	$M=25$	$M=75$	$M=10$
Llama-3.1-8B	0.76	2.34	15.24	32.88	104.30	63.45
Phi-4	1.42	3.84	23.27	59.90	167.59	166.76
Qwen2.5-7B	0.79	2.96	18.89	45.64	124.50	47.52

## F. Prompts

As discussed in section 6, all of the models in our experiments are instruction-tuned. For SPIDER, we use the prompt from (Loula et al., 2025), which is based on the (Sun et al., 2023). For BBH, we use the prompt template from (Polo et al., 2024). The detailed prompt templates for SPIDER, Big-Bench Hard (Word Sorting), JSON Schema are given below.

**F.1. JSON Schema**

```
# Prompt 1
[
  {
    'role': 'system',
    'content': 'You need to generate a JSON object that matches the schema below.
    ↪ Output the JSON object on a single line. DO NOT use multiple lines and DO NOT
    ↪ output any other text.'
  },
  {'role': 'user', 'content': '<example schema input string>'},
  {'role': 'assistant', 'content': '<example JSON output string>'},
  {'role': 'user', 'content': json.dumps(schema)},
]
# Prompt 2
[
  {
    'role': 'system',
    'content': 'Task: JSON object generation from schema specification.\n
    Input: JSON Schema (draft-04 or later)\n
    Output: Valid JSON object satisfying all schema constraints\n
    Format: Single-line JSON, no extraneous text'
  },
  {'role': 'user', 'content': '<example schema input string>'},
  {'role': 'assistant', 'content': '<example JSON output string>'},
  {'role': 'user', 'content': json.dumps(schema)},
]
```

**F.2. Big-Bench Hard (Word Sorting)**

```
# Prompt 1
[
  {
    'role': 'system',
    'content': 'You are a helpful assistant that sorts words in alphabetical order.
    ⇨ Your task is to take a list of words and return them sorted alphabetically.
    ⇨ Alphabetical order means sorting words from A to Z, comparing character by
    ⇨ character from left to right. For example, \'apple\' comes before \'banana\', and
    ⇨ \'cat\' comes before \'dog\''. When words start with the same letter, compare the
    ⇨ next letters. Output ONLY the sorted words separated by commas, with no additional
    ⇨ text, explanation, or commentary. Do not include any prefixes, suffixes, or extra
    ⇨ formatting - just the comma-separated sorted words.'
  },
  {
    'role': 'user',
    'content': 'Sort the following words in alphabetical order.\n\nInput: <list of
    ⇨ words>\nOutput:'
  }
]
# Prompt 2
[
  {
    'role': 'system',
    'content': 'You are a helpful assistant that sorts words in alphabetical order.
    ⇨ Your task is to take a list of words and return them sorted alphabetically. Output
    ⇨ ONLY the sorted words separated by commas, with no additional text, explanation,
    ⇨ or commentary.'
  },
  {'role': 'user', 'content': '<example input string> ->'},
  {'role': 'assistant', 'content': '<example target string>'},
  {'role': 'user', 'content': '<list of words> ->'}
]
```

## E.3. SPIDER

```

# Prompt 1
[
  {
    'role': 'system',
    'content': 'You are a coding assistant helping an analyst answer questions over
↳ business data in SQL. More specifically, the analyst provides you a database
↳ schema (tables in the database along with their column names and types) and asks a
↳ question about the data that can be solved by issuing a SQL query to the database.
↳ In response, you write the SQL statement that answers the question. You do not
↳ provide any commentary or explanation of what the code does, just the SQL
↳ statement ending in a semicolon.'
  },
  {
    'role': 'user',
    'content': 'Here is a database schema:\n\n<Table(Columns) Schema String> Please
↳ write me a SQL statement that answers the following question: <target question>\n
↳ nRemember, DO NOT provide any commentary or explanation of what the code does,
↳ just the SQL statement ending in a semicolon.'
  }
]
# Prompt 2
[
  {
    'role': 'system',
    'content': 'You are a coding assistant helping an analyst answer questions over
↳ business data in SQL. More specifically, the analyst provides you a database
↳ schema (tables in the database along with their column names and types) and asks a
↳ question about the data that can be solved by issuing a SQL query to the database.
↳ In response, you write the SQL statement that answers the question. You do not
↳ provide any commentary or explanation of what the code does, just the SQL
↳ statement ending in a semicolon.\n Here is the database schema for all following
↳ queries: \n\n<Columns=[]+FK Schema String>'
  },
  {
    'role': 'user',
    'content': 'Please write me a SQL statement that answers the following question:
↳ <example question>\n\nRemember, DO NOT provide any commentary or explanation of
↳ what the code does, just the SQL statement ending in a semicolon.'
  },
  {
    'role': 'assistant',
    'content': '<example SQL query>;'
  },
  {
    'role': 'user',
    'content': 'Please write me a SQL statement that answers the following question:
↳ <target question>\n\nRemember, DO NOT provide any commentary or explanation of
↳ what the code does, just the SQL statement ending in a semicolon.'
  }
]

```

Table 4. Comparison of  $f$ -ensemble functions (token-level SMC). **Bold**: highest average expected accuracy in column. †: non-overlapping 95% CIs with best baseline. Shaded: strongest single-prompt baseline.

Method	JSON Schema			BBH (Word Sorting)			SPIDER (Text-to-SQL)		
	Qwen	Phi	Llama	Qwen	Phi	Llama	Qwen	Phi	Llama
Prompt 1	95.6 $\pm$ 0.8	83.5 $\pm$ 1.9	86.3 $\pm$ 1.6	13.9 $\pm$ 1.0	27.7 $\pm$ 1.2	38.6 $\pm$ 1.5	40.0 $\pm$ 1.5	24.2 $\pm$ 1.5	38.4 $\pm$ 1.8
Prompt 2	93.8 $\pm$ 0.9	79.5 $\pm$ 5.6	84.3 $\pm$ 2.5	5.8 $\pm$ 0.9	24.3 $\pm$ 1.5	36.5 $\pm$ 1.9	53.6 $\pm$ 1.0	34.5 $\pm$ 1.7	36.3 $\pm$ 1.7
min	95.7 $\pm$ 0.4	<b>87.4<math>\pm</math>0.3</b> †	<b>88.9<math>\pm</math>1.1</b>	<b>15.3<math>\pm</math>2.0</b>	<b>28.2<math>\pm</math>1.1</b>	<b>42.3<math>\pm</math>0.9</b> †	<b>51.2<math>\pm</math>1.8</b>	<b>34.2<math>\pm</math>0.7</b>	<b>41.9<math>\pm</math>1.4</b> †
Product	<b>96.0<math>\pm</math>0.2</b>	86.4 $\pm$ 1.0	88.5 $\pm$ 1.0	15.2 $\pm$ 1.4	27.6 $\pm$ 1.2	40.9 $\pm$ 0.7†	50.9 $\pm$ 1.1	30.8 $\pm$ 0.1	41.7 $\pm$ 1.7†
Mixture	95.3 $\pm$ 0.8	81.3 $\pm$ 0.5	85.1 $\pm$ 1.3	9.8 $\pm$ 1.0	26.5 $\pm$ 0.0	37.4 $\pm$ 0.7	45.9 $\pm$ 0.6	29.4 $\pm$ 0.1	38.2 $\pm$ 1.6
max	95.2 $\pm$ 0.2	79.3 $\pm$ 1.1	83.7 $\pm$ 1.6	9.1 $\pm$ 1.0	25.4 $\pm$ 1.3	34.7 $\pm$ 1.4	45.9 $\pm$ 0.7	29.5 $\pm$ 0.1	37.9 $\pm$ 1.7

## G. Additional Results

### G.1. Detailed Ensembling Results

Complementarily to the condensed results shown in Table 2, we provide a version that is aggregated by ensembling method Table 4 which provides more detail on Figure 2, as well as the complete set of results in Table 5.

### G.2. Prompt Performance Overlap and Resulting Ensemble Performance

Complementing our discussion in §6.2, we examine how base model agreement affects ensemble performance. Fig. 4 plots per-sample expected accuracy under each prompt, with color indicating product ensemble accuracy and marker opacity distinguishing samples where the ensemble exceeds the best single-prompt baseline.

The results show that ensembles primarily improve performance on samples where prompts perform moderately (the diagonal), rather than those where one prompt dominates. This aligns with the mechanics of consensus-seeking: when experts disagree, the product ensemble’s gains are limited; however, when both partially succeed, the ensemble effectively concentrates probability on their intersection.

The pattern varies across models. For Llama, substantial mass lies along the diagonal, providing ample opportunity for ensemble gains. In contrast, Qwen exhibits more polarized behavior: samples tend to cluster near the axes (one prompt succeeds, the other fails) or in corners (both succeed or both fail), leaving fewer samples on the diagonal, where ensembling may help. This may explain why Qwen shows smaller ensemble improvements in Table 5.

### G.3. Particle Study

Finally, in Figure 5, Figure 6 and Figure 7, we plot the approximation quality as a function of the number of particles. As expected, as the number of particles increases, the approximation quality improves and variance reduces. Visually, we see that the increase in approximation quality saturates at around 10 to 25 particles for the evaluated scenarios. Following prior work by Loula et al. (2025), and to balance inference time with approximation cost, we choose to evaluate all setups using 10 particles.

### G.4. Additional Correlation Computations

Complementing Figure 3, we provide complete plots for all models and datasets in Figure 8, Figure 9 and Figure 10, alongside the average per-sample Spearman correlation in Table 6. Note that these correlation values differ: the table reports the average per-sample correlation, whereas the figures display the correlation across the entire dataset using  $z$ -normalized values to account for sample difficulty.

Table 5. Table reporting expected ensemble and base model accuracy at equal model weights, 10 particles with 95% confidence intervals evaluated across 5 seeds. For cross-model ensembling, we choose the prompt which has the best overall average base performance across models.

$f$ -Ensemble	Big-Bench Hard (Word Sorting)			SPIDER (Text-to-SQL)			JSON Schema		
	Qwen	phi	Llama	Qwen	phi	Llama	Qwen	phi	Llama
Prompt 1	13.9 $\pm$ 1.0	27.7 $\pm$ 1.2	38.6 $\pm$ 1.5	40.0 $\pm$ 1.5	24.2 $\pm$ 1.5	38.4 $\pm$ 1.8	95.6 $\pm$ 0.8	83.5 $\pm$ 1.9	86.3 $\pm$ 1.6
Prompt 2	5.8 $\pm$ 0.9	24.3 $\pm$ 1.5	36.5 $\pm$ 1.9	53.6 $\pm$ 1.0	34.5 $\pm$ 1.7	36.3 $\pm$ 1.7	93.8 $\pm$ 0.9	79.5 $\pm$ 5.6	84.3 $\pm$ 2.5
min, Token Local	15.0 $\pm$ 2.3	26.8 $\pm$ 5.1	45.0 $\pm$ 2.9	52.6 $\pm$ 1.4	36.0 $\pm$ 3.4	43.2 $\pm$ 2.1	95.4 $\pm$ 2.3	85.0 $\pm$ 1.5	87.2 $\pm$ 3.1
min, Token SMC	15.3 $\pm$ 2.0	28.2 $\pm$ 1.1	42.3 $\pm$ 0.9	51.2 $\pm$ 1.8	34.2 $\pm$ 0.7	41.9 $\pm$ 1.4	95.7 $\pm$ 0.4	87.4 $\pm$ 0.3	88.9 $\pm$ 1.1
min, Byte SMC	15.5 $\pm$ 0.1	23.8 $\pm$ 1.5	34.0 $\pm$ 1.4	47.8 $\pm$ 1.7	34.5 $\pm$ 0.9	41.5 $\pm$ 2.0	92.8 $\pm$ 1.0	87.5 $\pm$ 0.7	88.9 $\pm$ 1.4
min, Cross-Model Byte SMC	•29.4 $\pm$ 1.7• •27.6 $\pm$ 1.6•	•40.0 $\pm$ 2.8• •27.6 $\pm$ 1.6•		•50.9 $\pm$ 2.3• •53.4 $\pm$ 1.9•	•37.6 $\pm$ 1.7• •53.4 $\pm$ 1.9•		•90.8 $\pm$ 1.3• •83.6 $\pm$ 1.9•	•76.6 $\pm$ 3.0• •83.6 $\pm$ 1.9•	
Product, Token Local	14.8 $\pm$ 2.4	27.2 $\pm$ 5.1	43.2 $\pm$ 6.0	49.4 $\pm$ 2.9	32.0 $\pm$ 2.3	43.6 $\pm$ 3.4	95.4 $\pm$ 0.7	87.2 $\pm$ 4.4	88.6 $\pm$ 4.4
Product, Token SMC	15.2 $\pm$ 1.4	27.6 $\pm$ 1.2	40.9 $\pm$ 0.7	50.9 $\pm$ 1.1	30.8 $\pm$ 0.1	41.7 $\pm$ 1.7	96.0 $\pm$ 0.2	86.4 $\pm$ 1.0	88.5 $\pm$ 1.0
Product, Byte SMC	13.9 $\pm$ 1.9	22.9 $\pm$ 0.8	33.9 $\pm$ 1.8	48.3 $\pm$ 2.1	30.1 $\pm$ 3.1	42.4 $\pm$ 0.9	92.6 $\pm$ 0.6	87.4 $\pm$ 1.1	88.4 $\pm$ 0.7
Product, Cross-Model Byte SMC	•32.6 $\pm$ 1.1• •35.1 $\pm$ 3.9•	•41.1 $\pm$ 1.0• •35.1 $\pm$ 3.9•		•51.7 $\pm$ 2.9• •55.5 $\pm$ 1.1•	•39.1 $\pm$ 3.0• •55.5 $\pm$ 1.1•		•92.6 $\pm$ 0.9• •81.9 $\pm$ 3.7•	•74.8 $\pm$ 4.6• •81.9 $\pm$ 3.7•	
Mixture, Token Local	9.6 $\pm$ 3.0	25.8 $\pm$ 5.8	41.2 $\pm$ 6.5	45.6 $\pm$ 3.7	28.4 $\pm$ 4.8	39.4 $\pm$ 6.3	95.2 $\pm$ 3.2	82.0 $\pm$ 4.7	83.4 $\pm$ 3.5
Mixture, Token SMC	9.8 $\pm$ 1.0	26.5 $\pm$ 0.0	37.4 $\pm$ 0.7	45.9 $\pm$ 0.6	29.4 $\pm$ 0.1	38.2 $\pm$ 1.6	95.3 $\pm$ 0.8	81.3 $\pm$ 0.5	85.1 $\pm$ 1.3
Mixture, Byte SMC	7.9 $\pm$ 7.0	19.3 $\pm$ 0.5	26.0 $\pm$ 1.2	40.2 $\pm$ 3.3	25.1 $\pm$ 7.4	37.0 $\pm$ 2.2	92.5 $\pm$ 0.9	78.2 $\pm$ 4.2	86.1 $\pm$ 1.0
Mixture, Cross-Model Byte SMC	•16.7 $\pm$ 5.6• •17.9 $\pm$ 0.3•	•18.7 $\pm$ 4.4• •17.9 $\pm$ 0.3•		•39.5 $\pm$ 2.4• •39.1 $\pm$ 2.3•	•30.2 $\pm$ 1.7• •39.1 $\pm$ 2.3•		•83.7 $\pm$ 1.8• •88.3 $\pm$ 0.9•	•85.1 $\pm$ 1.3• •88.3 $\pm$ 0.9•	
max, Token Local	8.6 $\pm$ 3.8	24.6 $\pm$ 5.8	37.5 $\pm$ 6.7	45.8 $\pm$ 4.2	28.4 $\pm$ 4.4	38.0 $\pm$ 4.3	96.4 $\pm$ 0.7	79.4 $\pm$ 4.5	82.4 $\pm$ 3.2
max, Token SMC	9.1 $\pm$ 1.0	25.4 $\pm$ 1.3	34.7 $\pm$ 1.4	45.9 $\pm$ 0.7	29.5 $\pm$ 0.1	37.9 $\pm$ 1.7	95.2 $\pm$ 0.2	79.3 $\pm$ 1.1	83.7 $\pm$ 1.6
max, Byte SMC	8.2 $\pm$ 0.6	18.8 $\pm$ 1.9	24.2 $\pm$ 1.9	40.7 $\pm$ 3.6	27.9 $\pm$ 2.1	37.4 $\pm$ 3.8	92.1 $\pm$ 1.6	76.0 $\pm$ 4.3	86.1 $\pm$ 1.2
max, Cross-Model Byte SMC	•15.1 $\pm$ 0.1• •17.2 $\pm$ 2.1•	•17.5 $\pm$ 1.5• •17.2 $\pm$ 2.1•		•35.8 $\pm$ 2.3• •35.3 $\pm$ 4.6•	•33.3 $\pm$ 2.3• •35.3 $\pm$ 4.6•		•83.1 $\pm$ 1.8• •88.7 $\pm$ 1.1•	•85.2 $\pm$ 1.0• •88.7 $\pm$ 1.1•	

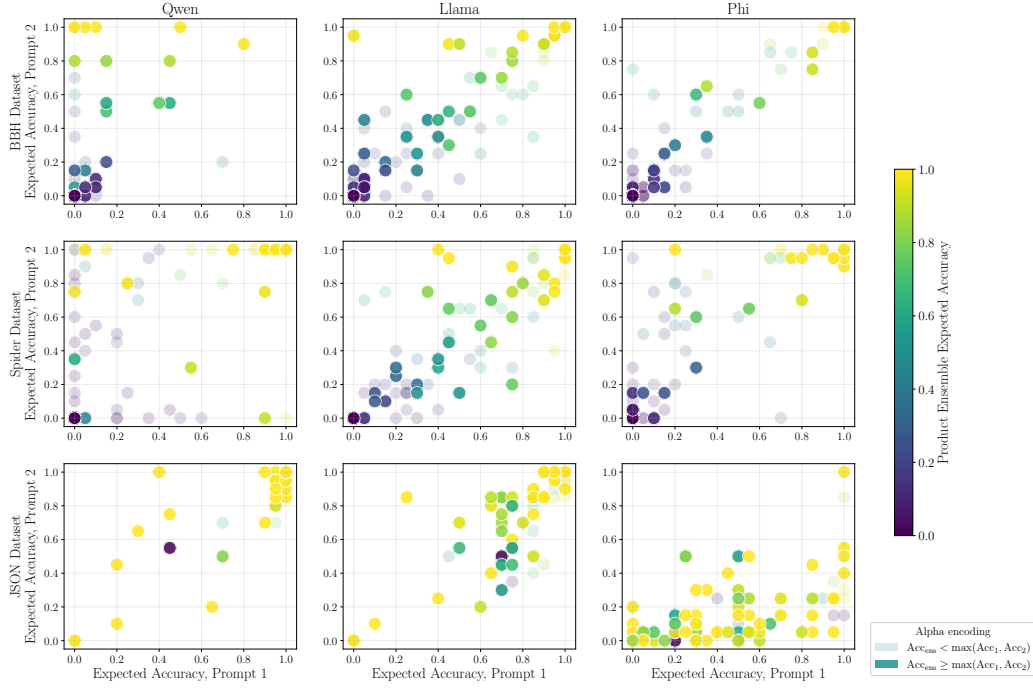


Figure 4. Scatter plots comparing expected accuracy of two prompt templates for all datasets and models. Color indicates product ensemble (token-level SMC) expected accuracy. Points with higher alpha indicate cases where the ensemble exceeds the best single template. Marker size scales with the improvement margin.

Table 6. Average per-sample Spearman correlation ( $r$ ) between  $\log \hat{Z}$  and expected accuracy. Values are reported as the mean of sample-level correlations  $\pm$  standard error. Significance levels (\*\*\*)  $p < 0.001$ , (\*\*)  $p < 0.01$ , (\*)  $p < 0.05$ ) are determined via a one-sample  $t$ -test against zero. Note that these values deviate from those in Figure 3, Figure 8, Figure 10, Figure 9 because they are computed per sample and then averaged.

Method	BBH (Word Sorting)			SPIDER (Text-to-SQL)			JSON Schema		
	Qwen	Phi	Llama	Qwen	Phi	Llama	Qwen	Phi	Llama
min	0.01 $\pm$ 0.07	0.15 $\pm$ 0.04***	0.22 $\pm$ 0.04***	0.04 $\pm$ 0.03	-0.03 $\pm$ 0.03	0.09 $\pm$ 0.03**	0.08 $\pm$ 0.03*	0.12 $\pm$ 0.03***	0.12 $\pm$ 0.02***
Product	0.03 $\pm$ 0.06	0.18 $\pm$ 0.04***	0.28 $\pm$ 0.04***	0.08 $\pm$ 0.05	0.09 $\pm$ 0.05	0.16 $\pm$ 0.04***	0.16 $\pm$ 0.03***	0.21 $\pm$ 0.02***	0.31 $\pm$ 0.03***
Sum	0.03 $\pm$ 0.03	0.00 $\pm$ 0.03	-0.05 $\pm$ 0.02*	-0.03 $\pm$ 0.03	-0.03 $\pm$ 0.02	-0.02 $\pm$ 0.02	0.03 $\pm$ 0.03	-0.01 $\pm$ 0.02	-0.02 $\pm$ 0.02
max	-0.07 $\pm$ 0.06	-0.01 $\pm$ 0.04	-0.14 $\pm$ 0.04***	-0.05 $\pm$ 0.03	-0.09 $\pm$ 0.03**	0.04 $\pm$ 0.02	-0.05 $\pm$ 0.04	-0.05 $\pm$ 0.02*	-0.01 $\pm$ 0.02

## Ensembling Language Models with Sequential Monte Carlo

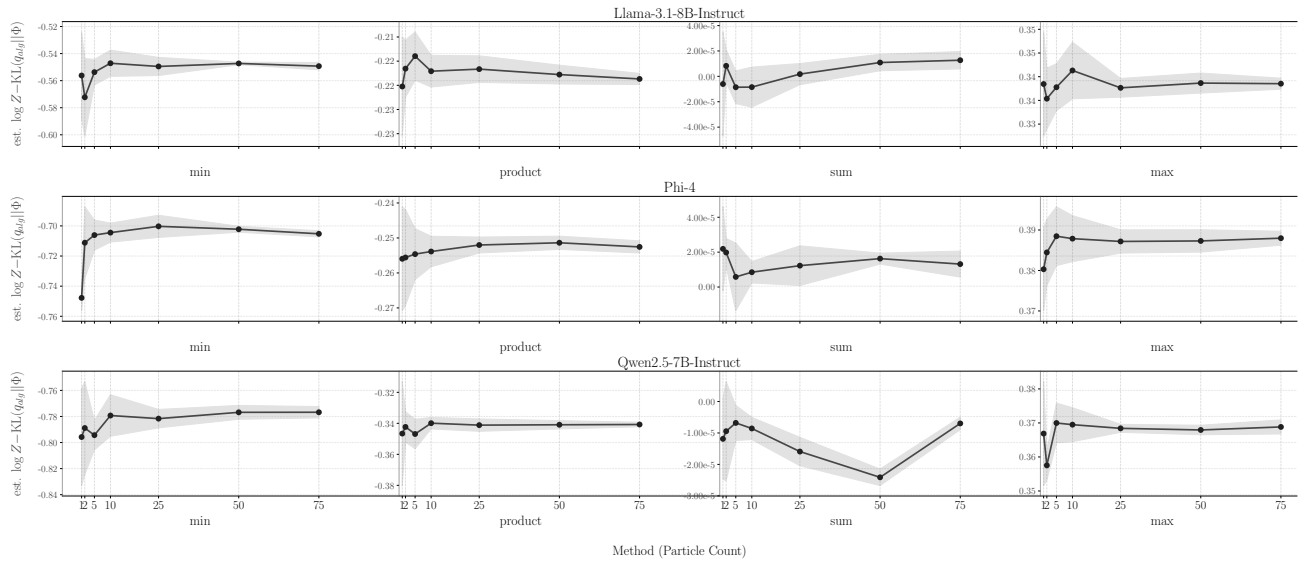


Figure 5. Particle study for JSON. We evaluate the approximation quality estimate  $\mathbb{E}[\log \hat{Z}]$  as a function of the number of particles being used for SMC.

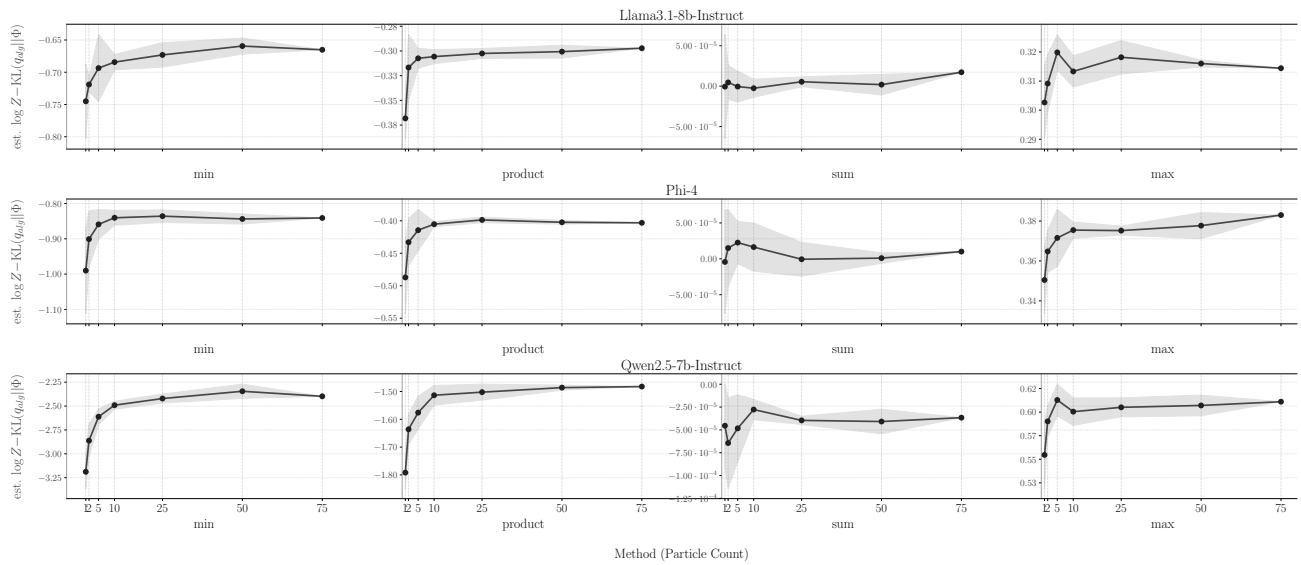


Figure 6. Particle study for BBH. We evaluate the approximation quality estimate  $\mathbb{E}[\log \hat{Z}]$  as a function of the number of particles being used for SMC.

## Ensembling Language Models with Sequential Monte Carlo

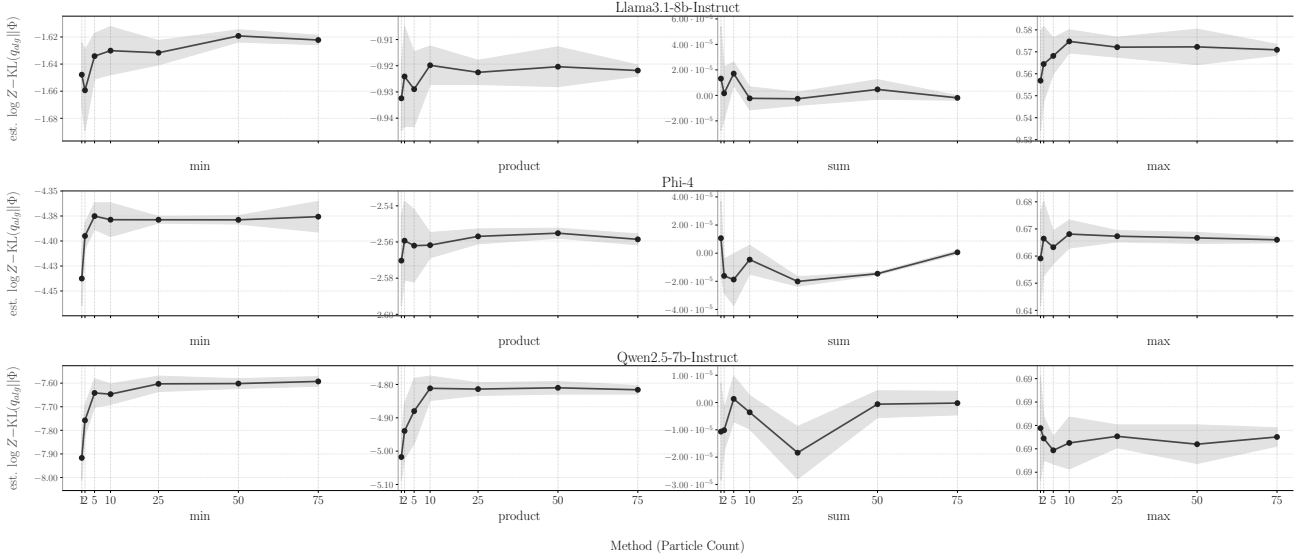


Figure 7. Particle study for SPIDER. We evaluate the approximation quality estimate  $\mathbb{E}[\log \hat{Z}]$  as a function of the number of particles being used for SMC.

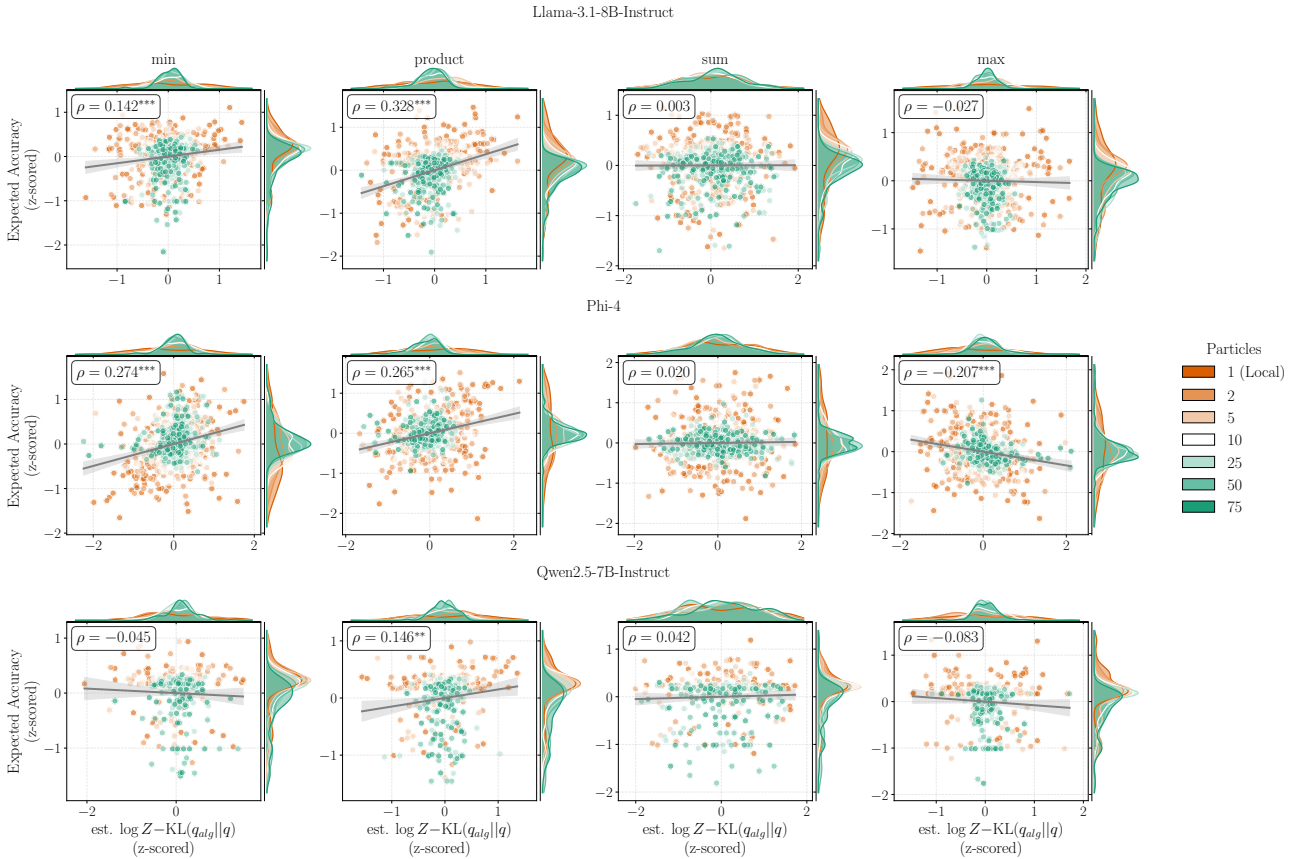


Figure 8. Relationship between expected accuracy and the estimated log marginal likelihood,  $\log \hat{Z}$ , on JSON for all models. Each datapoint represents (sample, particle) configurations aggregated across seeds. Both metrics are z-scored per example to normalize for variations in problem difficulty and scale. Points are colored by the number of particles used for estimation. Marginal plots display the kernel density estimates for the respective axes. The grey line and shaded band indicate a linear regression fit with a 95% confidence interval. Pearson correlation coefficients  $\rho$  are annotated in the top-left (\*\*\*)  $p < 0.001$ , (\*)  $p < 0.05$ .

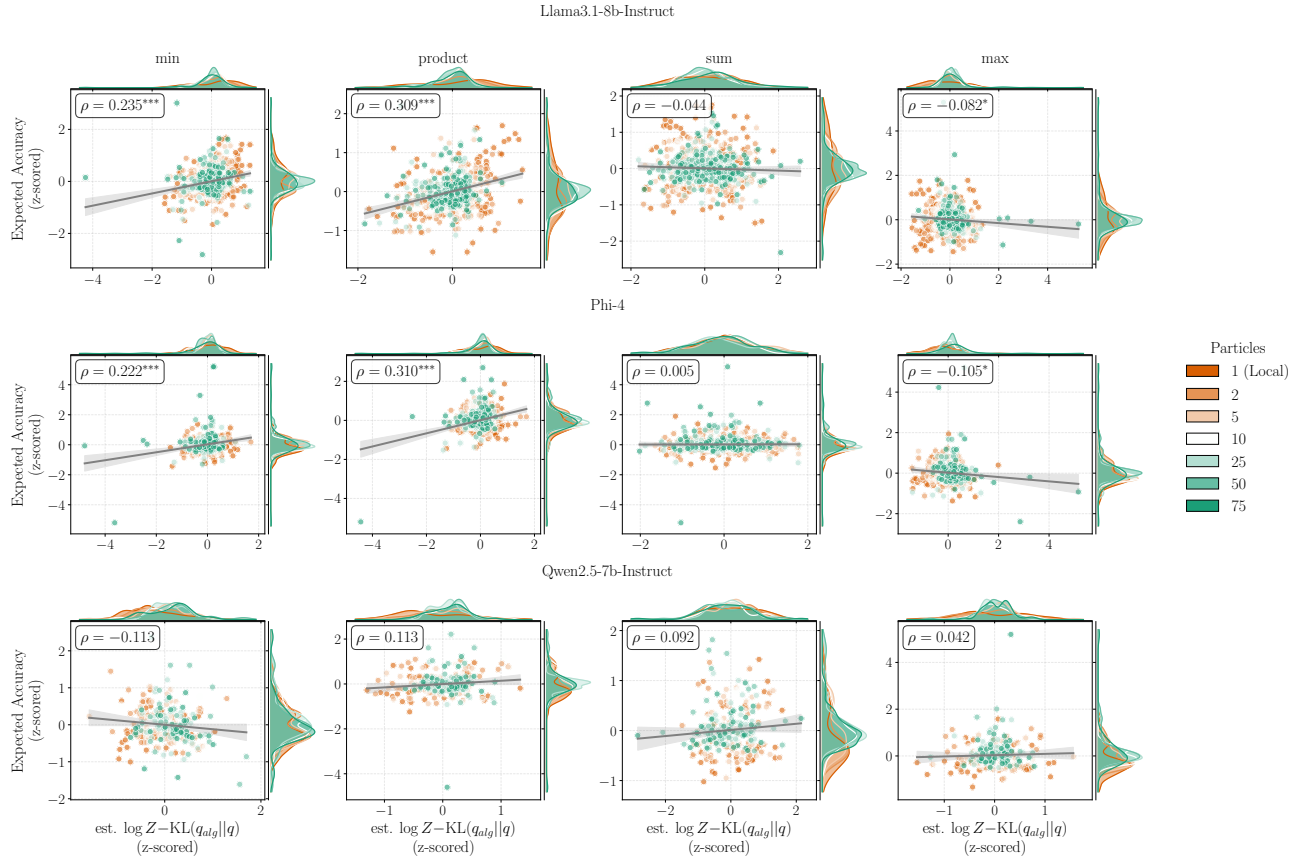


Figure 9. Relationship between expected accuracy and the estimated log marginal likelihood,  $\log \hat{Z}$ , on BBH for all models. Each datapoint represents (sample, particle) configurations aggregated across seeds. Both metrics are z-scored per example to normalize for variations in problem difficulty and scale. Points are colored by the number of particles used for estimation. Marginal plots display the kernel density estimates for the respective axes. The grey line and shaded band indicate a linear regression fit with a 95% confidence interval. Pearson correlation coefficients  $\rho$  are annotated in the top-left (\*\* $p < 0.001$ , \* $p < 0.05$ ).

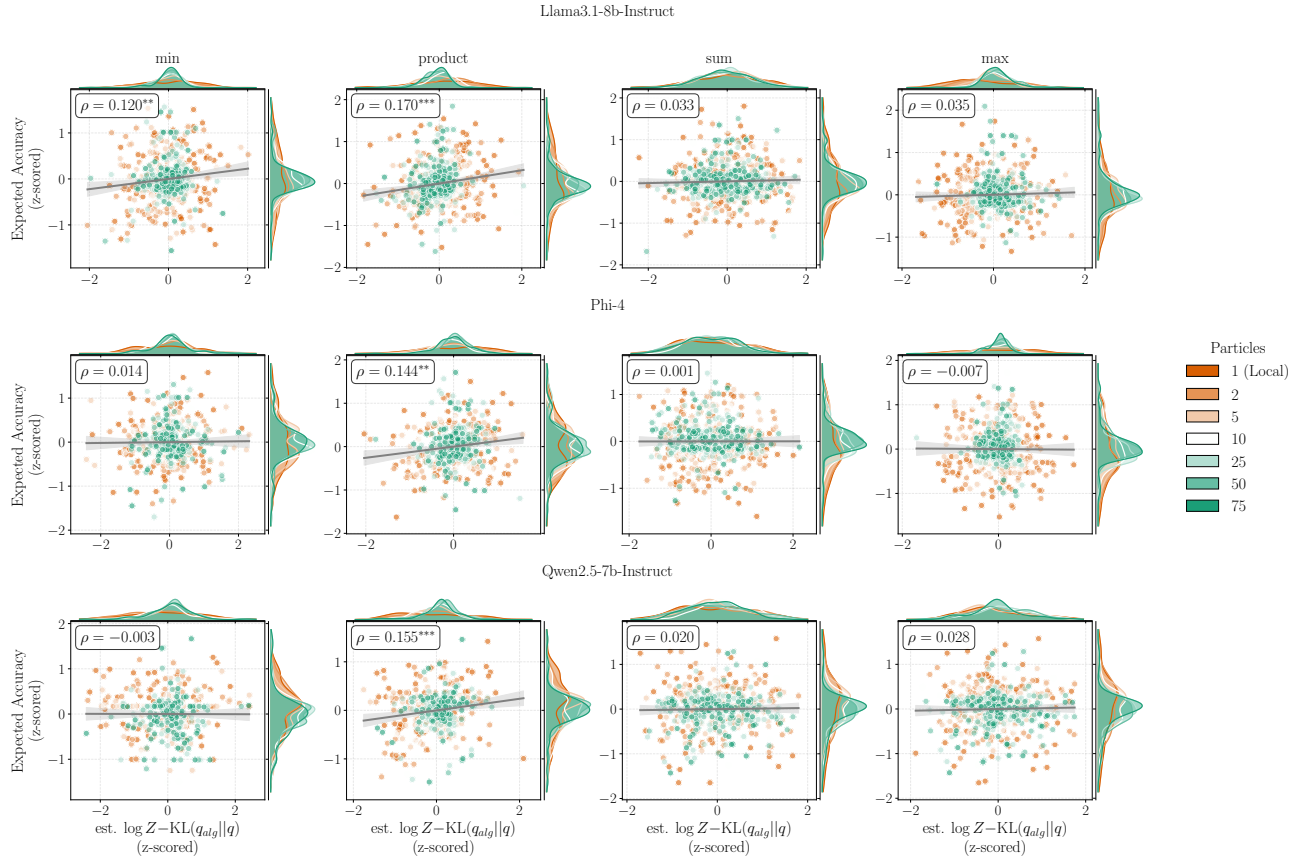


Figure 10. Relationship between expected accuracy and the estimated log marginal likelihood,  $\log \hat{Z}$ , on SPIDER for all models. Each datapoint represents (sample, particle) configurations aggregated across seeds. Both metrics are z-scored per example to normalize for variations in problem difficulty and scale. Points are colored by the number of particles used for estimation. Marginal plots display the kernel density estimates for the respective axes. The grey line and shaded band indicate a linear regression fit with a 95% confidence interval. Pearson correlation coefficients  $\rho$  are annotated in the top-left (\*\* $p < 0.001$ , \* $p < 0.05$ ).